

# Continuum Strong QCD: Confinement and Dynamical Chiral Symmetry Breaking

C.D. Roberts

*Physics Division, Bldg. 203, Argonne National Laboratory, Argonne IL 60439-4843, USA.*

**ABSTRACT:** Continuum strong QCD is the application of models and continuum quantum field theory to the study of phenomena in hadronic physics, which includes; e.g., the spectrum of QCD bound states and their interactions. Herein I provide a Dyson-Schwinger equation perspective, focusing on qualitative aspects of confinement and dynamical chiral symmetry breaking in cold, sparse QCD, and also elucidating consequences of the axial-vector Ward-Takahashi identity and features of the heavy-quark limit.

**KEYWORDS:** Bethe-Salpeter Equation, Confinement, Dynamical Chiral Symmetry Breaking, Dyson-Schwinger Equations, Hadron Physics, Heavy-quark Physics.

## Table of Contents

1. Introduction .....	1
2. Quark Propagator .....	2
(2.1) <i>Gluon Propagator</i> .....	4
(2.2) <i>Quark-gluon Vertex</i> .....	5
3. Dynamical Chiral Symmetry Breaking ..	5
4. Confinement .....	10
(4.1) <i>Three-dimensional QED</i> .....	11
5. Gap Equation's Kernel .....	13
(5.1) <i>Critical Interaction Tension</i> .....	17
6. Gluon DSE .....	17
7. Bethe-Salpeter Equation .....	20
(7.1) <i>Heavy-quark Limit</i> .....	23
8. Epilogue .....	25
9. References .....	25

## 1. Introduction

A primary goal in continuum strong QCD is to develop an intuitive understanding of the spectrum and interactions of hadrons in terms of QCD's elementary degrees of freedom. In addressing this an efficacious strategy is to employ a single framework in calculating a prodigious number of observables. With the aim being an elucidation of hadronic structure and nonperturbative aspects of QCD, a focus on the electroweak interactions of hadrons is most useful because in this case the probe is well understood and the features of the hadronic target are unambiguously under scrutiny. Both confinement and dynamical chiral symmetry breaking (DCSB) play key roles in determining these features, and are the main themes of this discourse.

As reviewed in Ref. [1], the last decade has seen a modest renaissance in the use of Dyson-Schwinger equations (DSEs) [2]: in exploring their formal foundation and in their phenomenological application. They provide the medium for this discussion.

The DSEs are a nonperturbative means of analysing a quantum field theory. Derived from a theory's Euclidean space generating functional, they are an enumerable infinity of coupled inte-

gral equations whose solutions are the  $n$ -point Schwinger functions [Euclidean Green functions], which are the same matrix elements estimated in numerical simulations of lattice-QCD. In theories with elementary fermions, the simplest of the DSEs is the *gap* equation, which is basic to studying dynamical symmetry breaking in systems as disparate as ferromagnets, superconductors and QCD. The gap equation is a good example because it is familiar and has all the properties that characterise each DSE: its solution is a 2-point function [the fermion propagator] while its kernel involves higher  $n$ -point functions; e.g., in a gauge theory, the kernel is constructed from the gauge-boson 2-point function and fermion-gauge-boson vertex, a 3-point function; a weak-coupling expansion yields all the diagrams of perturbation theory; and solved self-consistently, the solution of the gap equation exhibits nonperturbative effects unobtainable at any finite order in perturbation theory; e.g., dynamical symmetry breaking.

The coupling between equations; i.e., the fact that the equation for a given  $m$ -point function always involves at least one  $n > m$ -point function, necessitates a truncation of the tower of DSEs in order to define a tractable problem. One systematic and familiar truncation is a weak coupling expansion to reproduce perturbation theory. However, that precludes the study of non-perturbative phenomena and hence something else is needed for the investigation of strongly interacting systems and bound state phenomena.

In analysing the ferromagnetic transition, the Hartree-Fock approximation yields qualitatively reliable information and in QCD its analogue: the rainbow truncation, has proven efficacious. However, *a priori* it can be difficult to judge whether a given truncation will yield reliable results and a systematic improvement is not always obvious. It is here that some model-dependence enters but that is not new, being typical in the study of strongly-interacting few- and many-body systems.

To proceed with the DSEs one just employs a truncation and explores its consequences, applying it to different systems and constraining it, where possible, by comparisons with experimental data, and also with other theoretical ap-

proaches on their common domain of application. In this way a reliable truncation can be identified, and then attention paid to understanding the keystone of its success and improving its foundation. This pragmatic approach has proven rewarding in strong QCD, not least because a correctly-executed weak coupling expansion is guaranteed to match onto perturbation theory so that modelling is restricted to the infrared domain.

## 2. Quark Propagator

Obviously it is only possible to study DCSB in theories with a well-defined chiral limit. Asymptotically free theories such as QCD are in this class. A useful starting point for any discussion of DCSB is the renormalised quark-DSE [see App. A for the Euclidean metric conventions used herein]:

$$S(p)^{-1} = Z_2 (i\gamma \cdot p + m_{\text{bare}}) + Z_1 \int_q^\Lambda g^2 D_{\mu\nu}(p-q) \frac{\lambda^a}{2} \gamma_\mu S(q) \Gamma_\nu^a(q, p), \quad (2.1)$$

where  $D_{\mu\nu}(k)$  is the renormalised dressed-gluon propagator,  $\Gamma_\nu^a(q; p)$  is the renormalised dressed-quark-gluon vertex,  $m_{\text{bare}}$  is the  $\Lambda$ -dependent current-quark bare mass that appears in the Lagrangian and  $\int_q^\Lambda := \int^\Lambda d^4q / (2\pi)^4$  represents mnemonically a *translationally-invariant* regularisation of the integral, with  $\Lambda$  the regularisation mass-scale. The final step in any calculation is to remove the regularisation by taking the limit  $\Lambda \rightarrow \infty$ .

Using a translationally invariant regularisation makes possible the preservation of Ward-Takahashi identities, which is crucial; e.g., in studying DCSB [3]. One implementation well-suited to a nonperturbative solution of the DSE is Pauli-Villars regularisation, in which quarks interact with an additional massive gluon-like vector boson: mass  $\sim \Lambda$ , that decouples as  $\Lambda \rightarrow \infty$  [4]. An alternative is a numerical implementation of dimensional regularisation, which, although more cumbersome, can provide the necessary check of scheme-independence [5].

In Eq. (2.1),  $Z_1(\zeta^2, \Lambda^2)$  and  $Z_2(\zeta^2, \Lambda^2)$  are the quark-gluon-vertex and quark wave function

renormalisation constants, which depend on the renormalisation point,  $\zeta$ , and the regularisation mass-scale, as does the mass renormalisation constant

$$Z_m(\zeta^2, \Lambda^2) = Z_4(\zeta^2, \Lambda^2)/Z_2(\zeta^2, \Lambda^2), \quad (2.2)$$

with the renormalised mass given by

$$m(\zeta) := m_{\text{bare}}(\Lambda)/Z_m(\zeta^2, \Lambda^2). \quad (2.3)$$

Although I have suppressed the flavour label,  $S$ ,  $\Gamma_\mu^a$  and  $m_{\text{bare}}$  depend on it. However, one can always use a flavour-independent renormalisation scheme, which I assume herein, and hence all the renormalisation constants are flavour-independent [4].

The solution of Eq. (2.1) has the form

$$S(p) = \frac{1}{i\gamma \cdot p A(p^2, \zeta^2) + B(p^2, \zeta^2)}, \quad (2.4)$$

$$= \frac{Z(p^2, \zeta^2)}{i\gamma \cdot p + M(p^2, \zeta^2)}. \quad (2.5)$$

The functions  $A(p^2, \zeta^2)$ ,  $B(p^2, \zeta^2)$  embody all the effects of vector and scalar quark-dressing induced by the quark's interaction with its own gluon field. The ratio:  $M(p^2, \zeta^2)$ , is the quark mass function and a *pole* mass; i.e., the on-shell mass, would be the solution of

$$m_{\text{pole}}^2 - M^2(p^2 = -m_{\text{pole}}^2, \zeta^2) = 0. \quad (2.6)$$

A widely posed conjecture is that confinement rules out a solution of this equation [6], and that is discussed further in Sec. 4.

Equation (2.1) must be solved subject to a renormalisation [boundary] condition, and because the theory is asymptotically free it is practical and useful to impose the requirement that at a large spacelike  $\zeta^2$

$$S(p)^{-1}|_{p^2=\zeta^2} = i\gamma \cdot p + m(\zeta), \quad (2.7)$$

where  $m(\zeta)$  is the renormalised current-quark mass at the scale  $\zeta$ . By “large” here I mean  $\zeta^2 \gg \Lambda_{\text{QCD}}^2$  so that in quantitative, model studies extensive use can be made of matching with the results of perturbation theory. It is the ultra-violet stability of QCD; i.e., the fact that perturbation theory is valid at large spacelike momenta, that makes possible a straightforward definition

of the chiral limit. It also provides the starkest contrast to strong-coupling QED, whose rigorous definition remains an instructive challenge [2,7].

Multiplicative renormalisability in gauge theories entails that

$$\frac{A(p^2, \zeta^2)}{A(p^2, \tilde{\zeta}^2)} = \frac{Z_2(\zeta^2, \Lambda^2)}{Z_2(\tilde{\zeta}^2, \Lambda^2)} = A(\tilde{\zeta}^2, \zeta^2) = \frac{1}{A(\zeta^2, \tilde{\zeta}^2)} \quad (2.8)$$

and beginning with Ref. [8] this relation has been used efficaciously to build realistic *Ansätze* for the fermion–photon vertex in quenched QED. A systematic approach to such nonperturbative improvements is developing [9] and these improvements continue to provide intuitive guidance in QED, where they complement the perturbative calculation of the vertex [10]. They are also useful in exploring model dependence in QCD studies [11].

At one loop in QCD perturbation theory

$$Z_2(\zeta^2, \Lambda^2) = \left[ \frac{\alpha(\Lambda^2)}{\alpha(\zeta^2)} \right]^{-\gamma_F/\beta_1}, \quad (2.9)$$

$\gamma_F = \frac{2}{3}\xi$ ,  $\beta_1 = \frac{1}{3}N_f - \frac{11}{2}$ , and at this order the running strong-coupling is

$$\alpha(\zeta^2) = \frac{\pi}{-\frac{1}{2}\beta_1 \ln \left[ \zeta^2/\Lambda_{\text{QCD}}^2 \right]}. \quad (2.10)$$

In Landau gauge:  $\xi = 0$ , so  $Z_2 \equiv 1$  at one loop order. This, plus the fact that Landau gauge is a fixed point of the renormalisation group [Eq. (2.22)], makes it the most useful covariant gauge for model studies. It also underlies the quantitative accuracy of Landau gauge rainbow truncation estimates of the critical coupling in strong QED [12]. In a self consistent solution of Eq. (2.1),  $Z_2 \neq 1$  even in Landau gauge but, at large  $\zeta^2$ , the  $\zeta$ -dependence is very weak. However, as will become evident, in studies of realistic QCD models this dependence becomes significant for  $\zeta^2 \lesssim 1\text{--}2 \text{ GeV}^2$ , and is driven by the same effect that causes DCSB.

The dressed-quark mass function:  $M(p^2, \zeta^2) = B(p^2, \zeta^2)/A(p^2, \zeta^2)$ , is independent of the renormalisation point; i.e., with  $\zeta \neq \tilde{\zeta}$

$$M(p^2, \zeta^2) = M(p^2, \tilde{\zeta}^2) := M(p^2), \quad \forall p^2. \quad (2.11)$$

It is a function only of  $p^2/\Lambda_{\text{QCD}}^2$ , which is another constraint on models. At one loop order

the running [or renormalised] mass

$$m(\zeta) = M(\zeta^2) = \frac{\hat{m}}{\left(\frac{1}{2} \ln \left[\zeta^2 / \Lambda_{\text{QCD}}^2\right]\right)^{\gamma_m}}, \quad (2.12)$$

$\gamma_m = 12/(33 - 2N_f)$ , where  $\hat{m}$  is the renormalisation point independent current-quark mass, and the mass renormalisation constant is, Eq. (2.2),

$$Z_m(\zeta^2, \Lambda^2) = \left[\frac{\alpha(\Lambda^2)}{\alpha(\zeta^2)}\right]^{\gamma_m}. \quad (2.13)$$

The mass anomalous dimension,  $\gamma_m$ , is independent of the gauge parameter to all orders in perturbation theory and for two different quark flavours the ratio:

$$m_{f_1}(\zeta)/m_{f_2}(\zeta) = \hat{m}_{f_1}/\hat{m}_{f_2}, \quad (2.14)$$

which is independent of the renormalisation point and of the renormalisation scheme. The chiral limit is unambiguously defined by

$$\textbf{chiral limit : } \hat{m} = 0. \quad (2.15)$$

I reiterate now that a weak coupling expansion of Eq. (2.1) yields each of the diagrams in perturbation theory that contributes to the quark self energy. However, every one of those contributions to  $B(p^2, \zeta^2)$  is proportional to  $\hat{m}$  and therefore vanishes in the chiral limit; i.e.,  $B(p^2, \zeta^2) \equiv 0$  at every order in perturbation theory.

One finds, in fact, that in the chiral limit there is no scalar mass-like divergence in the calculation of the self energy. This is manifest in the quark DSE, with Eq. (2.1) capable of yielding, in addition to the perturbative result:  $B(p^2, \zeta^2) \equiv 0$ , a solution  $M(p^2) = B(p^2, \zeta^2)/A(p^2, \zeta^2) \neq 0$  that is power-law suppressed in the ultraviolet:  $M(p^2) \sim 1/p^2$ , guaranteeing *convergence* of the associated integral *without subtraction*. This is dynamical chiral symmetry breaking

$$\textbf{DCSB : } M(p^2) \neq 0 \text{ when } \hat{m} = 0. \quad (2.16)$$

As we shall see, in QCD this is possible if and only if the quark condensate is nonzero: the criteria are equivalent, and its existence places constraints on the kernel in Eq. (2.1), as discussed further in Sec. 5.

## 2.1 Gluon Propagator

That kernel is constructed from the dressed-gluon propagator and the dressed-quark-gluon vertex, and encodes in Eq. (2.1) all effects of the quark-quark interaction. In a covariant gauge the renormalised dressed-gluon propagator is

$$D_{\mu\nu}(k) = \left(\delta_{\mu\nu} - \frac{k_\mu k_\nu}{k^2}\right) \frac{d(k^2, \zeta^2)}{k^2} + \xi \frac{k_\mu k_\nu}{k^4}, \quad (2.17)$$

where  $d(k^2, \zeta^2) = 1/[1 + \Pi(k^2, \zeta^2)]$ , with  $\Pi(k^2, \zeta^2)$  the renormalised gluon vacuum polarisation for which the conventional renormalisation condition is

$$\Pi(\zeta^2, \zeta^2) = 0; \text{ i.e., } d(\zeta^2, \zeta^2) = 1. \quad (2.18)$$

For the dressed-gluon propagator, multiplicative renormalisability entails

$$\frac{d(k^2, \zeta^2)}{d(k^2, \tilde{\zeta}^2)} = \frac{Z_3(\tilde{\zeta}^2, \Lambda^2)}{Z_3(\zeta^2, \Lambda^2)} = d(\zeta^2, \tilde{\zeta}^2) = \frac{1}{d(\tilde{\zeta}^2, \zeta^2)}, \quad (2.19)$$

and at one loop in perturbation theory

$$Z_3(\zeta^2, \Lambda^2) = \left[\frac{\alpha(\Lambda^2)}{\alpha(\zeta^2)}\right]^{-\gamma_1/\beta_1}, \quad (2.20)$$

$\gamma_1 = \frac{1}{3}N_f - \frac{1}{4}(13 - 3\xi)$ . The gauge parameter is also renormalisation point dependent; i.e., the renormalised theory has a running gauge parameter. However, because of Becchi-Rouet-Stora [BRST or gauge] invariance, there is no new dynamical information in that: its evolution is completely determined by the gluon wave function renormalisation constant

$$\xi(\zeta^2) = Z_3^{-1}(\zeta^2, \Lambda^2) \xi_{\text{bare}}(\Lambda). \quad (2.21)$$

One can express  $\xi(\zeta^2)$  in terms of a renormalisation point invariant gauge parameter:  $\hat{\xi}$ , which is an overall multiplicative factor in the formula and hence

$$\textbf{Landau Gauge : } \hat{\xi} = 0 \Rightarrow \xi(\zeta^2) \equiv 0 \quad (2.22)$$

at all orders in perturbation theory; i.e., Landau gauge is a fixed point of the renormalisation group.

## 2.2 Quark-gluon Vertex

The other element of the kernel, the renormalised dressed-quark-gluon vertex, has the form

$$\Gamma_\nu^a(k, p) = \frac{\lambda^a}{2} \Gamma_\nu(k, p); \quad (2.23)$$

i.e., the colour matrix structure factorises. It is a fully amputated vertex, which means all the analytic structure associated with elementary excitations has been eliminated. To discuss this further I introduce the notion of a particle-like singularity.

A Particle-like Singularity is one of the form:  $P = k - p$ ,

$$\frac{1}{(P^2 + b^2)^\alpha}, \quad \alpha \in (0, 1]. \quad (2.24)$$

If the vertex possesses such a singularity then its  $P$ -dependence can be expressed via a non-negative spectral density, which is impossible if  $\alpha > 1$ .  $\alpha = 1$  is the ideal case of an isolated  $\delta$ -function distribution in the spectral densities and hence an isolated free-particle pole.  $\alpha \in (0, 1)$  corresponds to an accumulation at the particle pole of branch points associated with multiparticle production, as occurs with the electron propagator in QED because of photon dressing.

The dressed-quark-gluon vertex is a *fully amputated* 3-point function. Therefore in this case the presence of such a singularity would entail the existence of a flavour singlet composite [quark-antiquark bound state] with colour octet quantum numbers and mass  $m = b$ . [The bound state amplitude follows immediately from the associated homogeneous Bethe-Salpeter equation (BSE), which the singularity allows one to derive.] However, an excitation like this must not exist as an asymptotic state: that would violate the observational evidence of confinement. Hence, as discussed further on page 13, I conclude that the vertex should not exhibit a particle-like singularity, and any modelling of  $\Gamma_\mu^a(k, p)$  ought to be consistent with this constraint. [NB.  $\alpha > 1$  yields an admissible non-particle-like singularity.]

Expressing the Dirac structure of  $\Gamma_\nu(k, p)$  requires twelve independent scalar functions:

$$\Gamma_\nu(k, p) = \gamma_\nu F_1(k, p, \zeta) + \dots, \quad (2.25)$$

which it is not necessary to articulate fully herein. A pedagogical discussion of the perturbative calculation of  $\Gamma_\nu(k, p)$  can be found in Ref. [13] while Refs. [14,15] explore its nonperturbative structure and properties. I only make  $F_1(k, p, \zeta)$  explicit because the renormalisability of QCD entails that it alone is ultraviolet divergent. Defining

$$f_1(k^2, \zeta^2) := F_1(k, -k, \zeta), \quad (2.26)$$

the conventional renormalisation boundary condition is

$$f_1(\zeta^2, \zeta^2) = 1, \quad (2.27)$$

which is practical because QCD is asymptotically free. Multiplicative renormalisability entails

$$\begin{aligned} & \frac{f_1(k^2, \zeta^2)}{f_1(k^2, \tilde{\zeta}^2)} \\ &= \frac{Z_1(\zeta^2, \Lambda^2)}{Z_1(\tilde{\zeta}^2, \Lambda^2)} = f_1(\tilde{\zeta}^2, \zeta^2) = \frac{1}{f_1(\zeta^2, \tilde{\zeta}^2)}, \end{aligned} \quad (2.28)$$

and at one loop order

$$Z_1(\mu^2, \Lambda^2) = \left[ \frac{\alpha(\Lambda^2)}{\alpha(\mu^2)} \right]^{-\gamma_\Gamma/\beta_1}, \quad (2.29)$$

$$\gamma_\Gamma = \frac{1}{2} \left[ \frac{3}{4}(3 + \xi) + \frac{4}{3}\xi \right].$$

## 3. DCSB

At this point each element in the quark DSE, Eq. (2.1), is defined, with some of their perturbative properties elucidated, and the question is: “How does that provide an understanding of DCSB?” It is best answered using an example, in which the model-independent aspects are made clear.

The quark DSE is an integral equation and hence its elements must be known at all values of their momentum arguments, not just in the perturbative domain but also in the infrared. While the gluon propagator and quark-gluon vertex each satisfy their own DSE, that couples the quark DSE to other members of the tower of equations and hinders rather than helps in solving the gap equation. Therefore, as with all applications of the gap equation, one employs *Ansätze* for the interaction elements [ $D_{\mu\nu}(k)$  and  $\Gamma_\nu(k, p)$ ], constrained as much and on as large a domain as possible. This approach has a long

history in exploring QCD [2] and I illustrate it using the model of Ref. [4].

The renormalised dressed-ladder truncation of the quark-antiquark scattering kernel [4-point function] is

$$\bar{K}(p, q; P)_{tu}^{rs} = g^2(\zeta^2) D_{\mu\nu}(p - q) \quad (3.1)$$

$$\left[ \Gamma_\mu^a(p_+, q_+) S(q_+) \right]_{tr} \left[ S(q_-) \Gamma_\nu^a(q_-, p_-) \right]_{su},$$

where  $p_\pm = p \pm P/2$ ,  $q_\pm = q \pm P/2$ , with  $P$  the total momentum of the quark-antiquark pair, and although I use it now I have suppressed the  $\zeta$ -dependence of the Schwinger functions. From Eqs. (2.18-2.20) it follows that for  $Q^2 := (p - q)^2$  large and spacelike

$$d(Q^2, \zeta^2) = \frac{Z_3(\zeta^2, \Lambda^2)}{Z_3(Q^2, \Lambda^2)} d(\zeta^2, \zeta^2) \quad (3.2)$$

$$= \left[ \frac{\alpha(Q^2)}{\alpha(\zeta^2)} \right]^{\gamma_1/\beta_1} \quad (3.3)$$

$$\Rightarrow D_{\mu\nu}(p - q) = \left[ \frac{\alpha(Q^2)}{\alpha(\zeta^2)} \right]^{\gamma_1/\beta_1} D_{\mu\nu}^{\text{free}}(p - q). \quad (3.4)$$

Using this and analogous results for the other Schwinger functions then on the kinematic domain for which  $Q^2 \sim p^2 \sim q^2$  is large and space-like [ $g^2(\zeta^2) := 4\pi\alpha(\zeta^2)$ ]

$$\bar{K}(p, q; P)_{tu}^{rs} \approx 4\pi\alpha(Q^2) D_{\mu\nu}^{\text{free}}(p - q) \quad (3.5)$$

$$\left[ \frac{1}{2} \lambda^a \gamma_\mu S^{\text{free}}(q_+) \right]_{tr} \left[ S^{\text{free}}(q_-) \frac{1}{2} \lambda^a \gamma_\nu \right]_{su},$$

because Eqs. (2.9), (2.20) and (2.29) yield

$$\frac{2\gamma_F}{\beta_1} + \frac{\gamma_1}{\beta_1} - \frac{2\gamma_\Gamma}{\beta_1} = 1. \quad (3.6)$$

This is one way of understanding the origin of an often used *Ansatz* in studies of the gap equation; i.e., making the replacement

$$g^2 D_{\mu\nu}(k) \rightarrow 4\pi\alpha(k^2) D_{\mu\nu}^{\text{free}}(k) \quad (3.7)$$

in Eq. (2.1), and using the “rainbow truncation:”

$$\Gamma_\nu(q, p) = \gamma_\nu. \quad (3.8)$$

Equation (3.7) is often described as the “Abelian approximation” because the left- and right-hand-sides [r.h.s.] are *equal* in QED. In QCD, equality between the two sides cannot be obtained easily by a selective resummation of diagrams. As reviewed in Ref. [2], Eqs. (5.1-5.8),

it can only be achieved by enforcing equality between the renormalisation constants for the ghost-gluon vertex and ghost wave function:  $\tilde{Z}_1 = \tilde{Z}_3$ . A mutually consistent constraint, which follows formally from  $\tilde{Z}_1 = \tilde{Z}_3$ , is to enforce the Abelian Ward identity:  $Z_1 = Z_2$ . At one-loop this corresponds to neglecting the contribution of the 3-gluon vertex to  $\Gamma_\nu$ , in which case  $\gamma_\Gamma \rightarrow \frac{2}{3}\xi = \gamma_F$ . This additional constraint provides the basis for extensions of Eq. (3.8); i.e., using *Ansätze* for  $\Gamma_\nu$  that are consistent with the QED vector Ward-Takahashi identity; e.g., Refs. [11].

Arguments such as these inspire the following *Ansatz* for the kernel in Eq. (2.1) [4]:

$$Z_1 \int_q^\Lambda g^2 D_{\mu\nu}(p - q) \frac{\lambda^a}{2} \gamma_\mu S(q) \Gamma_\nu^a(q, p) \quad (3.9)$$

$$\rightarrow \int_q^\Lambda \mathcal{G}((p - q)^2) D_{\mu\nu}^{\text{free}}(p - q) \frac{\lambda^a}{2} \gamma_\mu S(q) \frac{\lambda^a}{2} \gamma_\nu,$$

with the ultraviolet behaviour of the so-called “effective coupling:”  $\mathcal{G}(k^2)$ , fixed by that of the running strong-coupling. Since it is not possible to calculate  $Z_1$  nonperturbatively without analysing the DSE for the dressed-quark-gluon vertex, this *Ansatz* absorbs it in the model effective coupling.

Equation (3.9) is a model for the product of the dressed-propagator and dressed-vertex and its definition is complete once the behaviour of  $\mathcal{G}(k^2)$  in the infrared is specified; i.e., for  $k^2 \lesssim 1\text{-}2\text{ GeV}^2$ . Reference [4] used

$$\frac{\mathcal{G}(k^2)}{k^2} = 8\pi^4 D \delta^4(k) + \frac{4\pi^2}{\omega^6} D k^2 e^{-k^2/\omega^2}$$

$$+ \frac{8\gamma_m \pi^2}{\ln \left[ \tau + \left( 1 + k^2/\Lambda_{\text{QCD}}^2 \right)^2 \right]} \mathcal{F}(k^2), \quad (3.10)$$

with  $\mathcal{F}(k^2) = [1 - \exp(-k^2/[4m_t^2])]/k^2$  and  $\tau = e^2 - 1$ . For  $N_f = 4$ ,  $\Lambda_{\text{QCD}}^{N_f=4} = 0.234\text{ GeV}$ .

The qualitative features of Eq. (3.10) are plain. The first term is an integrable infrared singularity [16] and the second is a finite-width approximation to  $\delta^4(k)$ , normalised such that it has the same  $\int d^4k$  as the first term. In this way the infrared strength is split into the sum of a zero-width and a finite-width piece. The last term in Eq. (3.10) is proportional to  $\alpha(k^2)/k^2$  at

large spacelike- $k^2$  and has no singularity on the real- $k^2$  axis.

There are ostensibly three parameters in Eq. (3.10):  $D$ ,  $\omega$  and  $m_t$ . However, in Ref. [4]  $\omega = 0.3 \text{ GeV}$  ( $= 1/[.66 \text{ fm}]$ ) and  $m_t = 0.5 \text{ GeV}$  ( $= 1/[.39 \text{ fm}]$ ) were fixed, and only  $D$  and the renormalised  $u = d$ - and  $s$ -current-quark masses were varied in an attempt to obtain a good description of low-energy  $\pi$ - and  $K$ -meson properties, using a renormalisation point  $\zeta = 19 \text{ GeV}$  that is large enough to be in the perturbative domain. [The numerical values of  $\omega$  and  $m_t$  are chosen so as to ensure that  $\mathcal{G}(k^2) \approx 4\pi\alpha(k^2)$  for  $k^2 > 2 \text{ GeV}^2$ . Minor variations in  $\omega$  and  $m_t$  can be compensated by small changes in  $D$ .] Such a procedure could self-consistently yield  $D = 0$ , which would indicate that agreement with observable phenomena precludes an infrared enhancement in the effective interaction. However, that was not the case and a good fit required

$$D = (0.884 \text{ GeV})^2, \quad (3.11)$$

with renormalised current-quark masses

$$m_{u,d}(\zeta) = 3.74 \text{ MeV}, \quad m_s(\zeta) = 82.5 \text{ MeV}, \quad (3.12)$$

which are in the ratio 1 : 22, and yielded, in MeV,

	$m_\pi$	$m_K$	$f_\pi$	$f_K$	
Calc. [4]	139	497	131	154	(3.13)
Expt. [17]	139	496	131	160	

and other quantities to be described below. An explanation of how this fit was accomplished requires a discussion of the homogeneous Bethe-Salpeter equation, which I postpone until Sec. 7. It is described in detail in Refs. [4,18]. Here I focus instead on describing the properties of the DSE solution obtained with these parameter values.

Using Eqs. (2.1-2.3) and (3.9) the gap equation can be written

$$S(p, \zeta)^{-1} = Z_2 i\gamma \cdot p + Z_4 m(\zeta) + \Sigma'(p, \Lambda), \quad (3.14)$$

with the regularised quark self energy

$$\Sigma'(p, \Lambda) := \int_q^\Lambda \mathcal{G}((p-q)^2) D_{\mu\nu}^{\text{free}}(p-q) \frac{\lambda^a}{2} \gamma_\mu S(q) \frac{\lambda^a}{2} \gamma_\nu. \quad (3.15)$$

When  $\hat{m} \neq 0$  the renormalisation condition, Eq. (2.7), is straightforward to implement. Writing

$$\Sigma'(p, \Lambda) := i\gamma \cdot p (A'(p^2, \Lambda^2) - 1) + B'(p^2, \Lambda^2), \quad (3.16)$$

which emphasises that these functions depend on the regularisation mass-scale,  $\Lambda$ , Eq. (2.7) entails

$$Z_2(\zeta^2, \Lambda^2) = 2 - A'(\zeta^2, \Lambda^2), \quad (3.17)$$

$$m(\zeta) = Z_2(\zeta^2, \Lambda^2) m_{\text{bm}}(\Lambda^2) + B'(\zeta^2, \Lambda^2) \quad (3.18)$$

so that

$$A(p^2, \zeta^2) = 1 + A'(p^2, \Lambda^2) - A'(\zeta^2, \Lambda^2), \quad (3.19)$$

$$B(p^2, \zeta^2) = m(\zeta) + B'(p^2, \Lambda^2) - B'(\zeta^2, \Lambda^2). \quad (3.20)$$

Multiplicative renormalisability requires that having fixed the solutions at a single renormalisation point,  $\zeta$ , their form at another point,  $\tilde{\zeta}$ , is given by

$$S^{-1}(p, \tilde{\zeta}) = \frac{Z_2(\tilde{\zeta}^2, \Lambda^2)}{Z_2(\zeta^2, \Lambda^2)} S^{-1}(p, \zeta). \quad (3.21)$$

This feature is evident in the solutions obtained in Ref. [4]. It means that, in evolving the renormalisation point to  $\tilde{\zeta}$ , the “1” in Eqs. (3.19) is replaced by  $Z_2(\tilde{\zeta}^2, \Lambda^2)/Z_2(\zeta^2, \Lambda^2)$ , and the “ $m(\zeta)$ ” by  $m(\tilde{\zeta})$ ; i.e., the “seeds” in the integral equation evolve according to the QCD renormalisation group. This is why Eq. (3.9) is called a “renormalisation-group-improved rainbow truncation.”

Returning to the chiral limit, it follows from Eqs. (2.2), (2.3), (2.12) and (2.15) that for  $\hat{m} = 0$

$$Z_2(\zeta^2, \Lambda^2) m_{\text{bare}}(\Lambda^2) = 0, \quad \forall \Lambda. \quad (3.22)$$

Hence, as remarked on page 4, there is no subtraction in the equation for  $B(p^2, \zeta^2)$ ; i.e., Eq. (3.19) becomes

$$B(p^2, \zeta^2) = B'(p^2, \Lambda^2), \quad \lim_{\Lambda \rightarrow \infty} B'(p^2, \Lambda^2) < \infty, \quad (3.23)$$

which is only possible if the mass function is at least  $1/p^2$ -suppressed. This is not the case in quenched strong-coupling QED, where the mass function behaves as [19]

$$\propto \cos(\text{const.} \ln[p^2/\zeta^2])/(p^2/\zeta^2)^{1/2}, \quad (3.24)$$

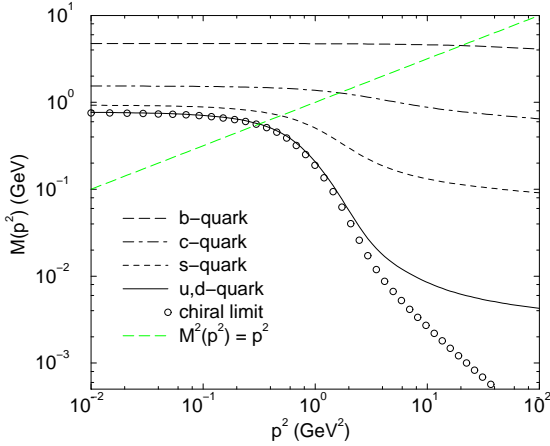


**Figure 1:** Quark mass function obtained as a solution of Eq. (2.1) using the model of Eqs. (3.9), (3.10), and current-quark masses, fixed at a renormalisation point  $\zeta = 19$  GeV:  $m_{u,d}^\zeta = 3.7$  MeV,  $m_s^\zeta = 82$  MeV,  $m_c^\zeta = 0.58$  GeV and  $m_b^\zeta = 3.8$  GeV. The indicated solutions of  $M^2(p^2) = p^2$  define the Euclidean constituent-quark mass,  $M_f^E$ , which takes the values:  $M_u^E = 0.56$  GeV,  $M_s^E = 0.70$  GeV,  $M_c^E = 1.3$  GeV,  $M_b^E = 4.6$  GeV. These values and their ratios are consistent with contemporary phenomenology; e.g., Refs.[17,20] (Figure adapted from Refs. [21,22].)

and that is the origin of the complications discussed in Refs. [2,5,7].

In Fig. 1 I present the renormalised dressed-quark mass function,  $M(p^2)$ , obtained by solving Eq. (3.14) using the model and parameter values of Ref. [4], Eqs. (3.9-3.12), and also in the chiral limit and with typical heavy-quark current-mass values.

In the presence of explicit chiral symmetry breaking Eq. (2.12) describes the form of  $M(p^2)$  for  $p^2 > \mathcal{O}(1 \text{ GeV}^2)$ . In the chiral limit, however, the ultraviolet behaviour is given by

$$M(p^2) \stackrel{\text{large-}p^2}{\sim} \frac{2\pi^2\gamma_m}{3} \frac{(-\langle\bar{q}q\rangle^0)}{p^2 \left( \frac{1}{2} \ln \left[ p^2 / \Lambda_{\text{QCD}}^2 \right] \right)^{1-\gamma_m}}, \quad (3.25)$$

where  $\langle\bar{q}q\rangle^0$  is the renormalisation-point-independent vacuum quark condensate. This behaviour too is characteristic of the QCD renormalisation group [23] and exhibits the power-law suppression anticipated on page 4. These results for the large- $p^2$  behaviour of the mass function are

model independent; i.e., they arise only because the DSE truncation is consistent with the QCD renormalisation group at one loop. (It has long been known that the truncation defined by Eq. (3.9) yields results in agreement with the QCD renormalisation group at one loop; e.g., Refs. [24].)

The gauge invariant expression for the renormalisation-point-dependent vacuum quark condensate was derived in Ref. [25]:

$$-\langle\bar{q}q\rangle_\zeta^0 := Z_4(\zeta^2, \Lambda^2) N_c \text{tr}_D \int_q^\Lambda S^0(q, \zeta), \quad (3.26)$$

where  $\text{tr}_D$  identifies a trace over Dirac indices only and the superscript “0” indicates the quantity was calculated in the chiral limit. Substituting Eq. (3.25) into Eq. (3.26), recalling that  $Z_4 = Z_m$  in Landau gauge and using Eq. (2.13) leads to the one-loop expression

$$\langle\bar{q}q\rangle_\zeta^0 = \left( \frac{1}{2} \ln \zeta^2 / \Lambda_{\text{QCD}}^2 \right)^{\gamma_m} \langle\bar{q}q\rangle^0. \quad (3.27)$$

Employing Eq. (2.12), this exemplifies the general result that

$$m(\zeta) \langle\bar{q}q\rangle_\zeta^0 = \hat{m} \langle\bar{q}q\rangle^0; \quad (3.28)$$

i.e., that this product is renormalisation point invariant and, importantly, it shows that the behaviour expressed in Eq. (3.25) is exactly that required for consistency with the gauge invariant expression for the quark condensate. A model, such as Ref. [26], in which the scalar projection of the chiral limit dressed-quark propagator falls faster than  $1/p^4$ , up to  $\ln$ -corrections, is only consistent with this quark condensate vanishing, and it is this condensate that appears in the current algebra expression for the pion mass [25], as discussed in connection with Eq. (7.8).

Equation (3.25) provides a reliable means of calculating the quark condensate because corrections are suppressed by powers of  $\Lambda_{\text{QCD}}^2 / \zeta^2$ . Analysing the asymptotic form of the numerical solution one finds

$$-\langle\bar{q}q\rangle^0 = (0.227 \text{ GeV})^3. \quad (3.29)$$

Using Eq. (3.27) one can define a one-loop evolved condensate

$$-\langle\bar{q}q\rangle_\zeta^0|_{\zeta=1 \text{ GeV}} := -(\ln [1 / \Lambda_{\text{QCD}}])^{\gamma_m} \langle\bar{q}q\rangle^0, \quad (3.30)$$

which takes the value

$$-\langle \bar{q}q \rangle_\zeta^0|_{\zeta=1 \text{ GeV}} = (0.241 \text{ GeV})^3. \quad (3.31)$$

This can be directly compared with the value of the quark condensate employed in contemporary phenomenological studies [27]:

$$(0.236 \pm 0.008 \text{ GeV})^3. \quad (3.32)$$

It was noted in Ref. [4] that increasing  $\omega \rightarrow 1.5\omega$  in  $\mathcal{G}(k^2)$  increases the calculated value in Eq. (3.30) by  $\sim 10\%$ ; i.e., the magnitude of the condensate is correlated with the degree of infrared enhancement/strength in the effective interaction. That is unsurprising because it has long been known that there is a critical coupling for DCSB; i.e., the kernel in the gap equation must have an integrated strength that exceeds some critical value [24]. This is true in all fermion-based studies of DCSB, a point discussed in more detail on page 17.

The renormalisation-point-invariant current-quark masses corresponding to the  $m_f(\zeta)$  in Fig. 1 are obtained in the following way: using Eq. (3.26), direct calculation from the chiral limit numerical solution gives

$$\langle \bar{q}q \rangle_{\zeta=19 \text{ GeV}}^0 = -(0.275 \text{ GeV})^3, \quad (3.33)$$

and hence from the values of  $m_f^\zeta \equiv m_f(\zeta)$  listed in Fig. 1 and Eqs. (3.28), (3.29), in MeV,

$$\begin{aligned} \hat{m}_{u,d} &= 6.60, & \hat{m}_s &= 147, \\ \hat{m}_c &= 1030, & \hat{m}_b &= 6760, \end{aligned} \quad (3.34)$$

from which also follow one-loop evolved values in analogy with Eq. (3.30):

$$\begin{aligned} m_{u,d}^{1 \text{ GeV}} &= 5.5, & m_s^{1 \text{ GeV}} &= 130, \\ m_c^{1 \text{ GeV}} &= 860, & m_b^{1 \text{ GeV}} &= 5700. \end{aligned} \quad (3.35)$$

Smaller values of the light-current-quark masses would require a larger value of the vacuum quark condensate in order to be consistent with light-meson properties.

Figure 1 highlights a number of qualitative aspects of the quark mass function. One is the difference in the ultraviolet between the behaviour of  $M(p^2)$  in the chiral limit and in the presence of explicit chiral symmetry breaking. In the infrared, however, the  $u, d$ -quark mass function

and the chiral limit solution are almost indistinguishable. The chiral limit solution is nonzero *only* because of the nonperturbative DCSB mechanism whereas the  $u, d$ -quark mass function is purely perturbative at  $p^2 > 20 \text{ GeV}^2$ . Hence the evolution to coincidence of the chiral-limit and  $u, d$ -quark mass functions makes clear the transition from the perturbative to the nonperturbative domain.

It is on this nonperturbative domain that  $A(p^2, \zeta^2)$  differs significantly from one. A concomitant observation is that the DCSB mechanism has a significant effect on the propagation characteristics of  $u, d, s$ -quarks. These aspects of the momentum-dependence of the scalar functions in the dressed-light-quark propagators have recently been confirmed in numerical simulations of lattice-QCD [28], as illustrated in the comparisons of Fig. 2.

Returning to Fig. 1, it is evident that the large current-quark mass of the  $b$ -quark almost entirely suppresses momentum-dependent dressing, so that  $M_b(p^2)$  is nearly constant on a substantial domain. This is true to a lesser extent for the  $c$ -quark but in both cases one observes that DCSB is not the dominant mass-generating mechanism.

A means of quantifying the effect of the DCSB mechanism on dressed-quark propagation characteristics is now obvious. One can introduce [21,22]:  $\mathcal{L}_f := M_f^E/m_f^\zeta$ , where  $M_f^E$  is the Euclidean constituent-quark mass, defined in Fig. 1 as the solution of

$$(M_f^E)^2 - M^2(p^2) = (M_f^E)^2, \zeta^2 = 0, \quad (3.36)$$

and this ratio takes the values

$$\frac{f}{\mathcal{L}_f} \left| \begin{array}{c|cccc} & u, d & s & c & b \\ \hline & 150 & 10 & 2.2 & 1.2 \end{array} \right. \quad (3.37)$$

The values are representative and definitive: for light-quarks  $\mathcal{L}_{q=u,d,s} \sim 10\text{--}100$ , while for heavy-quarks  $\mathcal{L}_{Q=c,b} \sim 1$ ; and highlight the existence of a mass-scale characteristic of DCSB:  $M_\chi$ . The propagation characteristics of a flavour with  $m_f^\zeta \leq M_\chi$  are significantly altered by the DCSB mechanism, while for flavours with  $m_f^\zeta \gg M_\chi$  momentum-dependent dressing is almost irrelevant. It is apparent and unsurprising that  $M_\chi \sim$

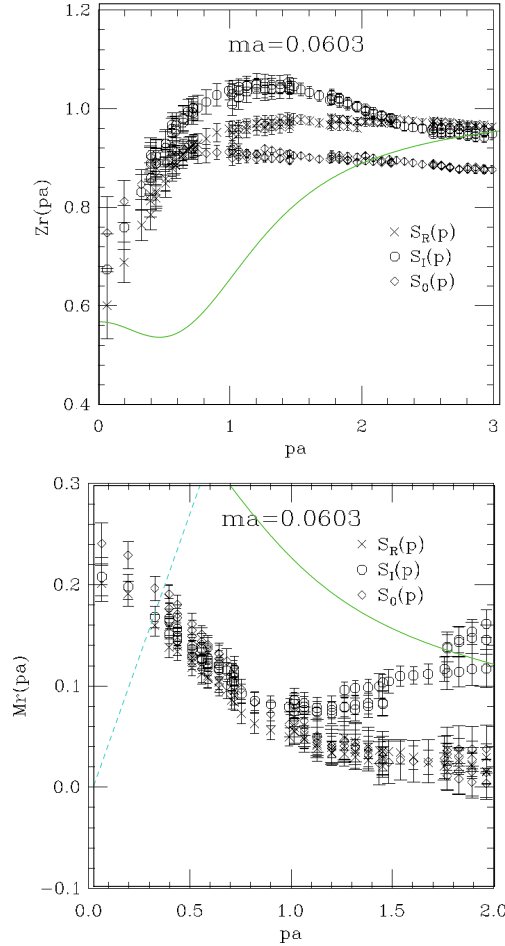


**Figure 2:** *Upper Panel:* Lattice result for  $Z(pa)$ ,  $a \simeq 2.0 \text{ GeV}^{-1}$  is the lattice spacing, calculated with  $ma = 0.0603$  [28], compared with the DSE analogue:  $Z(x)$ ,  $x$  is a dimensionless momentum variable, from the phenomenological algebraic model of Ref. [29]. The variation between the lattice results is an indication of extant numerical artefacts. The “dip” in  $Z(x)$  for  $x \simeq 0$  is a long-standing prediction of phenomenologically efficacious DSE studies. *Lower Panel:* Analogous plot for the mass function. Numerical artefacts are more significant in this case. Nevertheless the enhancement at small- $pa$ , indicative of DCSB, is clearly evident and in semi-quantitative agreement with that predicted by DSE studies. The dashed-line assists with estimating the Euclidean constituent-quark mass:  $\sim 200 \text{ MeV}$  in the lattice simulation and  $\sim 350$  in the phenomenological DSE model [29].

$0.2 \text{ GeV} \sim \Lambda_{\text{QCD}}$ . This feature of the dressed-quark mass function provides the foundation for a constituent-quark-like approximation in the

treatment of heavy-meson decays and transition form factors [22,30].

## 4. Confinement

To proceed it is necessary to discuss confinement and I begin with a definition. Confinement is the failure to directly observe coloured excitations in a detector: neither quarks nor gluons nor coloured composites. The contemporary hypothesis is stronger; i.e., coloured excitations cannot propagate to a detector. To ensure this it is sufficient that coloured  $n$ -point functions violate the axiom of reflection positivity [31], which is guaranteed if the Fourier transform of the momentum-space  $n$ -point Schwinger function is not a positive-definite function of its arguments.

Reflection positivity is one of a set of five axioms that must be satisfied if the given  $n$ -point function is to have a continuation to Minkowski space and hence an association with a physical, observable state. If an Hamiltonian exists for the theory but a given  $n$ -point function violates reflection positivity then the space of observable states, which is spanned by the eigenstates of the Hamiltonian, does not contain anything corresponding to the excitation(s) described by that Schwinger function.

The free boson propagator does not violate reflection positivity:

$$\Delta(x) := \int \frac{d^4 k}{(2\pi)^4} e^{ik \cdot x} \frac{1}{k^2 + m^2} \quad (4.1)$$

$$= \frac{m}{4\pi^2 x} K_1(mx). \quad (4.2)$$

Here  $x := (x \cdot x)^{1/2} > 0$  and  $K_1$  is the monotonically decreasing, strictly convex-up, non-negative modified Bessel function of the second kind. The same is true of the free fermion propagator:

$$S(x) = \int \frac{d^4 k}{(2\pi)^4} e^{ik \cdot x} \frac{m - i\gamma \cdot k}{k^2 + m^2} \quad (4.3)$$

$$= \frac{m^2}{4\pi^2 x} \left[ K_1(mx) + \frac{\gamma \cdot x}{x} K_2(mx) \right], \quad (4.4)$$

which is also positive definite.

The spatially averaged Schwinger function is a particularly insightful tool [32,33]. Consider the fermion and let  $T = x_4$  represent Euclidean

“time,” then

$$\begin{aligned}\sigma_S(T) &:= \int d^3x \frac{1}{4} \text{tr}_D S(\vec{x}, T) \\ &= \frac{1}{\pi} \int_0^\infty d\ell \frac{m}{\ell^2 + m^2} \cos(\ell T) \\ &= \frac{1}{2} e^{-mT}.\end{aligned}\quad (4.5)$$

Hence the free fermion’s mass can easily be obtained from the large  $T$  behaviour of the spatial average:

$$mT = -\lim_{T \rightarrow \infty} \ln \sigma_S(T). \quad (4.6)$$

[The boson analogy is obvious.] This is just the approach used to determine bound state masses in simulations of lattice-QCD.

For contrast, consider the dressed-gluon 2-point function obtained with [34]

$$d(k^2) = \frac{k^4}{k^4 + \gamma^4} \quad (4.7)$$

in Eq. (2.17)

$$\begin{aligned}D(x) &:= \int \frac{d^4k}{(2\pi)^4} e^{ik \cdot x} \frac{k^2}{k^4 + \gamma^4} \\ &= -\frac{\gamma}{4\pi^2 x} \left( \frac{d}{dz} \text{ker}(z) \right) \Big|_{z=\gamma x},\end{aligned}\quad (4.8)$$

where  $\text{ker}(z)$  is the oscillatory Thomson function.  $D(x)$  is not positive definite and hence a dressed-gluon 2-point function that vanishes at  $k^2 = 0$  violates the axiom of reflection positivity and is therefore not observable; i.e., the excitation it describes is confined.

At asymptotically large Euclidean distances

$$\begin{aligned}D(x) &\stackrel{x \rightarrow \infty}{\propto} \frac{\gamma^{1/2}}{x^{3/2}} e^{-\gamma x / \sqrt{2}} \\ &\times \left[ \cos\left(\frac{1}{\sqrt{2}}\gamma x + \frac{\pi}{8}\right) + \sin\left(\frac{1}{\sqrt{2}}\gamma x + \frac{\pi}{8}\right) \right].\end{aligned}\quad (4.10)$$

Comparing this with Eq. (4.1) one identifies a mass as the coefficient in the exponential:

$$m_D = \gamma / \sqrt{2}. \quad (4.11)$$

[NB. At large  $x$ ,  $K_1(x) \propto \exp(-x)/\sqrt{x}$ .] By an obvious analogy, the coefficient in the oscillatory term is the *lifetime* [34]:

$$\tau = 1/m_D. \quad (4.12)$$

Both the mass and lifetime are tied to the dynamically generated mass-scale  $\gamma$ , which, using

$$\frac{z}{z^2 + \gamma^4} = \frac{1}{2} \frac{1}{z + i\gamma^2} + \frac{1}{2} \frac{1}{z - i\gamma^2}, \quad (4.13)$$

is just the displacement of the complex conjugate poles from the real- $k^2$  axis.

It is a general result that the Fourier transform of a real function with complex conjugate poles is not positive definite. Hence the existence of such poles in a  $n$ -point Schwinger function is a sufficient condition for the violation of reflection positivity and thus for confinement.

The spatially averaged Schwinger function is also useful here.

$$\begin{aligned}D(T) &:= \int d^3x D(\vec{x}, T) \\ &= \frac{1}{2\gamma} e^{-\frac{1}{\sqrt{2}}\gamma T} \cos\left(\frac{1}{\sqrt{2}}\gamma T + \frac{\pi}{4}\right),\end{aligned}\quad (4.14)$$

and, generalising Eq. (4.6), one can define a  $T$ -dependent mass:

$$\begin{aligned}m(T)T &:= -\ln D(T) \\ &= \ln(2\gamma) + \frac{1}{\sqrt{2}}\gamma T - \ln \left[ \cos\left(\frac{1}{\sqrt{2}}\gamma T + \frac{\pi}{4}\right) \right].\end{aligned}\quad (4.15)$$

It exhibits periodic singularities whose frequency is proportional to the dynamical mass-scale that is responsible for the violation of reflection positivity. If a dressed-fermion 2-point function has complex conjugate poles it too will be characterised by a  $T$ -dependent mass that exhibits such behaviour.

#### 4.1 Three-dimensional QED

This reflection positivity criterion has been employed to very good effect in three dimensional QED [35]. First, some background. QED<sub>3</sub> is confining in the quenched truncation [36]. That is evident in the classical potential

$$\begin{aligned}V(r) &:= \int_{-\infty}^{\infty} dx_3 \int \frac{d^3k}{(2\pi)^3} e^{i\vec{k} \cdot \vec{x} + ik_3 x_3} \frac{e^2}{k^2} \\ &= \frac{e^2}{2\pi} \ln(e^2 r), \quad r^2 = x_1^2 + x_2^2,\end{aligned}\quad (4.16)$$

which describes the interaction between two static sources. [NB.  $e^2$  has the dimensions of mass in QED<sub>3</sub>.] It is a logarithmically growing potential, showing that the energy required to separate two charges is infinite. Furthermore,  $V(r)$

is just a one-dimensional average of the spatial gauge-boson 2-point Schwinger function and it is not positive definite, which indicates that the photon is also confined.

However, if now the photon vacuum polarisation tensor is evaluated at order  $e^2$  using  $N_f$  massless fermions then, with the notation of Eq. (2.17), the photon propagator is characterised by [37]

$$\frac{d(k^2)}{k^2} = \frac{1}{k^2 + \tilde{\alpha}k}, \text{ from } \Pi(k^2) = \frac{\tilde{\alpha}}{k}, \quad (4.17)$$

$\tilde{\alpha} = N_f e^2/8$ , and one finds [38]

$$V(r) = \frac{e^2}{4} [\mathbf{H}_0(\tilde{\alpha}r) - N_0(\tilde{\alpha}r)], \quad (4.18)$$

where  $\mathbf{H}_0(x)$  is a Struve function and  $N_0(x)$  a Neumann function, both of which are related to Bessel functions. In this case  $V(r)$  is positive definite, with the limiting cases

$$V(r) \stackrel{r \rightarrow 0}{\approx} -\ln(\tilde{\alpha}r), \quad V(r) \stackrel{r \rightarrow \infty}{\approx} \frac{e^2}{2\pi} \frac{1}{\tilde{\alpha}r}, \quad (4.19)$$

and confinement is lost in QED<sub>3</sub>. That is easy to understand: pairs of massless fermions cost no energy to produce and can propagate to infinity so they are very effective at screening the interaction.

With  $d(k^2) = 1/[1 + \Pi(k^2)]$  and sensible, physical constraints on the form of  $\Pi(k^2)$ , such as boundedness and vanishing in the ultraviolet, one can show that [39]

$$V(r) \stackrel{r \rightarrow \infty}{\approx} \frac{e^2}{2\pi} \frac{1}{1 + \Pi(0)} \ln(e^2 r) + \text{const.} + h(r), \quad (4.20)$$

where  $h(r)$  falls-off at least as quickly as  $1/r$ . Hence, the existence of a confining potential in QED<sub>3</sub> just depends on the value of the vacuum polarisation at the origin. In the quenched truncation,  $\Pi(0) = 0$  and the theory is logarithmically confining. With massless fermions,  $1/[1 + \Pi(0)] = 0$  and confinement is absent. Finally, when the vacuum polarisation is evaluated from a loop of massive fermions, whether that mass is obtained dynamically via the gap equation or simply introduced as an external parameter, one obtains  $\Pi(0) < \infty$  and hence a confining theory.

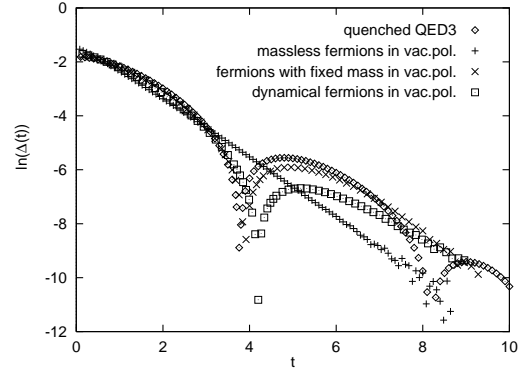


**Figure 3:**  $\Delta(T) := -\sigma_S(T)$  from Eq. (4.5) for QED<sub>3</sub> with 2 flavours of fermion. “Diamond:” confining, quenched theory; “plus,” massless fermions used to evaluate the photon vacuum polarisation tensor; “cross,” as before but with fixed-mass fermions; “box,” same again but fermions with a momentum-dependent mass function. (Adapted from Ref. [35].)

In Ref. [35] the QED<sub>3</sub> gap equation is solved for all four cases and the fermion propagator analysed. The results are summarised by Fig. 3. In the quenched theory, Eq. (4.16), the dressed-fermion 2-point function exhibits exactly those periodic singularities that, via Eq. (4.16), are indicative of complex conjugate poles. Hence this feature of the 2-point function, tied to the violation of reflection positivity, is a clear signal of confinement in the theory. That is emphasised further by a comparison with the theory that is unquenched via massless fermions in the vacuum polarisation, Eq. (4.17). As I have described, that theory is not confining and in this case  $\sigma_S(T)$  has the noninteracting, unconfined free particle form in Eq. (4.5). The difference could not be more stark. The remaining two cases exhibit the periodic singularities that signal confinement, just as they should based on Eq. (4.20).

At this point I note that any concern that the presence of complex conjugate singularities in coloured  $n$ -point functions leads to a violation of causality is misguided. Microscopic causality only constrains the commutativity of operators, and products thereof, that represent elements in the space of observable particle states; i.e., the space spanned by eigenstates of the Hamiltonian. Since Schwinger functions that violate reflection

positivity do not have a continuation into that space there can be no question of violating causality. It is only required that  $\mathcal{S}$ -matrix elements that describe colour-singlet to colour-singlet transitions should satisfy the axioms, including reflection positivity.

The violation of reflection positivity by coloured  $n$ -point functions is a sufficient condition for confinement. However, it is not necessary, as the example of planar, two-dimensional QCD shows [40]. There the fermion two-point function exhibits particle-like singularities but the colour singlet meson bound state amplitudes, obtained from a Bethe-Salpeter equation, vanish at momenta coincident with the constituent-fermion mass shell. This excludes the pinch singularities that would otherwise lead to bound state break-up and liberation of the constituents. It is a realisation of confinement via a failure of the cluster decomposition property [CDP] [31,41].

The CDP is a requirement that the difference between the vacuum expectation value of a product of fields and all products of vacuum expectation values of subsets of these fields must vanish faster than any power. [This is modified slightly in theories, like QED, with a massless, asymptotic state: the photon in this case.] It can be understood as a statement about charge screening and its failure means that, irrespective of the separation between sources, the interaction between them is never negligible. That is an appealing, intuitive representation of confinement. Failure of the CDP is an implicit basis for confinement in the bulk of QCD potential models; e.g., Refs. [42].

## 5. Gap Equation's Kernel

Strong interaction phenomena are characterised by DCSB and colour confinement. At low energy, DCSB is the more important; for example, in its absence the  $\pi$ - and  $\rho$ -mesons would be nearly degenerate and at the simplest observational level that would lead to a markedly different line of nuclear stability. These phenomena can be related to the infrared behaviour of elementary Schwinger functions in QCD and in this section I elucidate some constraints they place on this behaviour.

In Eq. (3.9) I described an *Ansatz* for the kernel in the quark DSE and used it to elaborate on the phenomenon of DCSB, arguing that a good description of light-meson observables *requires* the kernel to exhibit a significant enhancement in the infrared, Eq.(3.11). An obvious question is: "How far-reaching is this result?"

In general, as is clear from Eq. (3.9), the kernel is a product of two terms: the dressed-gluon propagator and the dressed-quark-gluon vertex. For  $k^2 \geq 1\text{--}2\text{ GeV}^2$  a perturbative analysis for this product is reliable and Eq. (3.9) becomes an identity with  $\mathcal{G}(k^2) \rightarrow 4\pi\alpha(k^2)$ . This means that any model-dependence in the *Ansatz* is constrained to the infrared domain:  $k^2 < 1\text{--}2\text{ GeV}^2$ .

In contemporary DSE applications to QCD it is common to build *Ansätze* for the higher  $n$ -point dressed-Schwinger functions and employ them in developing intuition about the simpler functions. Section 3 provides an illustration. In pursuing this certain constraints must be obeyed.

Of particular interest here is the dressed-quark-gluon vertex, which is a fully-amputated 3-point Schwinger function. It satisfies an integral equation that takes the form of an inhomogeneous Bethe-Salpeter equation. The kernel involves  $K$ : the fully-amputated, quark-antiquark scattering kernel, which by definition does not contain quark-antiquark to single gauge-boson annihilation diagrams, such as would describe the leptonic decay of the pion, nor diagrams that become disconnected by cutting one quark and one antiquark line. It also involves the scattering kernels for:  $q\bar{q}$  to 2-gluon,  $K^{2g}$ ;  $q\bar{q}$  to ghost-antighost,  $K^{ghgh}$ ; and  $q\bar{q}$  to 3-gluon,  $K^{3g}$ , and also by definition none of these can contain single-gluon intermediate states. Hence, just as in the chiral limit a massless pole in the pseudovector vertex signals the presence of a massless [pion] bound state, a massless, particle-like singularity [see Eq. (2.24)] in  $\Gamma_\nu(q, p)$  signals the presence of a colour-octet bound state in the scattering matrices:  $M := K/[1 - (SS)K]$ ;  $M^{2g} := K^{2g}/[1 - (DD)K^{2g}]$ ; etc. As no such coloured bound states has been observed, one must be sceptical of calculations or *Ansätze* for any of the Schwinger functions that entail a particle-like singularity in this vertex. [NB. It is internally inconsistent to interpret as confined a gluon

whose 2-point function violates reflection positivity whilst simultaneously asserting that a particle-like singularity in a coloured irreducible 3-point function does not describe an asymptotic state.]

The same objection applies to particle-like singularities in the fully-amputated, dressed-3-gluon vertex, and all like coloured  $n$ -point functions. This anticipates the result of an estimate [43] of the 3-gluon vertex via a numerical simulation of lattice-QCD, which shows no evidence for a singularity of any kind.

Rejecting particle-like singularities in  $\Gamma_\mu(q, p)$ , the possibility of an enhancement in the kernel of the gap equation can be discussed solely in terms of the behaviour of the dressed-gluon propagator, which in Landau gauge can be written [cf. Eq. (2.17)]

$$D_{\mu\nu}(k) = \left( \delta_{\mu\nu} - \frac{k_\mu k_\nu}{k^2} \right) \Delta(k^2), \quad (5.1)$$

$$\Delta(k^2) := \frac{1}{k^2} \mathcal{P}(k^2). \quad (5.2)$$

The question I posed at the beginning of this section can now be rephrased as: “Do observable strong interaction phenomena *necessarily* require

$$\mathcal{P}(k^2) \gg 1 \text{ for } 1 \lesssim k^2/\Lambda_{\text{QCD}}^2 \lesssim 10?” \quad (5.3)$$

[ $\Lambda_{\text{QCD}}^{N_f=4} = 234 \text{ MeV}$ .] NB. Herein I do not canvass the possibility that an irreducible vertex has a non-particle-like singularity; i.e., a singularity of the form  $(k^2)^{-\alpha}$ ,  $\alpha > 1$ . While that evades the constraint I have elucidated, there is no indication of such behaviour in any study to date.

I do not have an answer to the question in Eq. (5.3) but the alternatives can be explored. The antithesis is the extreme possibility that

$$\mathcal{P}(k^2 = 0) = 0, \quad \mathcal{P}(k^2) \leq 1 \quad \forall k^2, \quad (5.4)$$

which was canvassed in Refs. [34]. [“Extreme” because it corresponds to a screening of the fermion-fermion interaction, as familiar in an electro-dynamical plasma, rather than the antiscreening often discussed in zero-temperature chromodynamics.]

References [34] proposed solving the DSEs via rational polynomial *Ansätze* for the one-particle irreducible components of the Schwinger

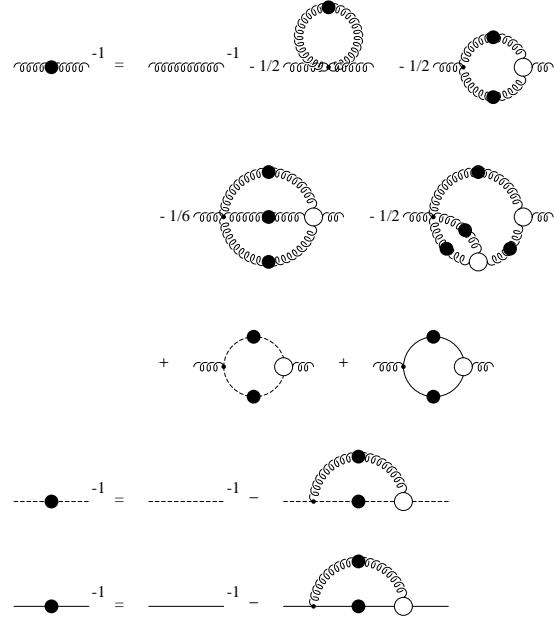


**Figure 4:** From top to bottom, depictions of the DSEs for the gluon (spring), ghost (dashed-line) and quark (solid-line) 2-point functions. Following convention, a filled circle denotes a fully dressed propagator and an open circle, a one-particle irreducible vertex; e.g., the open circle in the first line represents the dressed-three-gluon vertex. The figure illustrates the interrelation between elements in the tower of DSEs: the gluon propagator appears in the DSE for the quark and ghost propagator; the ghost and quark propagator in the DSE for the gluon, etc. (Adapted from Ref. [44].)

functions. This method attempts to preserve aspects of the organising principle of perturbation theory in truncating the DSEs. In connection with the gluon DSE, depicted in Fig. 4, these studies employed a truncation that, for simplicity: retains only the first, third and sixth diagrams on the r.h.s. of the first equation in Fig. 4; neglects the last [fermion] equation; and employs the leading order solution of the ghost equation, which has the appearance of the massless free propagator:  $\sim 1/k^2$ . In this approach the *Ansätze* for the 3-gluon and quark-gluon vertices exhibit *ideal* particle-like poles [ $\alpha = 1$  in Eq. (2.24)]. Since these poles are an essential element of the solution procedure then, in the absence of a physically sensible interpretation or explanation of them, one could simply reject this result.

Alternatively, one can suppose that Eq. (5.4) is more robust than the procedure employed to motivate it and explore the phenomenological consequences of the conjecture [34]:

$$\mathcal{P}_S(k^2) := k^4/(k^4 + b^4), \quad (5.5)$$

where  $b$  is a dynamically generated mass scale. Following this approach it was found that if there are no particle-like singularities in the quark-gluon vertex,  $\Gamma_\nu(q, p)$ , then  $\mathcal{P}_S(k^2)$  is unable to confine quarks [32,46] and  $b$  must be fine-tuned to very small values:

$$b < b_c \simeq \Lambda_{\text{QCD}}, \quad (5.6)$$

if DCSB is to occur [32,45–48]. It is therefore apparent that Eq. (5.4) is phenomenologically difficult to maintain. [NB. Achieving DCSB by requiring  $b \sim 0$  is indicative of the *dynamical evasion* of Eq. (5.4) since  $\mathcal{P}_S(k^2) \rightarrow 1$  rapidly for small values of  $b$ .]

Nevertheless, the hypothesis has been explored in studies [49] of the dressed-gluon 2-point function using numerical simulations of lattice-QCD.  $\mathcal{P}(k^2 = 0)$  is necessarily finite in simulations on a finite lattice because of the inherent infrared cutoff. Thus one can only truly determine  $\mathcal{P}(k^2 \sim 0)$  by considering the behaviour of the numerical result in both the countable limit of infinitely many lattice sites and the continuum limit.

The form  $\mathcal{P}_S(k^2)$  does not provide as good a fit to the lattice data as an alternative form, which in the countable limit is

$$\mathcal{P}_L(k^2) := \frac{k^2}{M^2 + Z k^2 (k^2 a^2)^\eta}, \quad (5.7)$$

$0 < k^2 < 0.6/a^2 \sim 50 \Lambda_{\text{QCD}}^2$ , where  $1/a \approx 2.0 \text{ GeV}$  is the inverse lattice spacing,  $Z \approx 0.1$ ,  $\eta \approx 0.53$ , and  $M \approx 0.16 \text{ GeV}$ . This takes the maximum value

$$\mathcal{P}_L(k^2 = 21 \Lambda_{\text{QCD}}^2) = 13.6 \quad (5.8)$$

and corresponds to a less extreme alternative to Eq. (5.4), which I shall characterise as

$$\mathcal{P}(k^2 = 0) = 0, \max(\mathcal{P}(k^2)) \lesssim \mathcal{O}(10). \quad (5.9)$$

The feature  $\mathcal{P}(k^2 = 0) = 0$  is critically dependent on whether or not  $M$  is nonzero. It appears to be nonzero in the countable limit but,

as emphasised in Ref. [49], the behaviour of  $M$  (and  $\eta$ ) in the continuum limit is unknown. [NB. All existing lattice-QCD simulations of the gluon propagator; e.g., Ref. [50], yield fitted forms that lie in the class specified by Eq. (5.9). A dressed-gluon propagator satisfying Eq. (5.4) automatically satisfies Eq. (5.9).]

The phenomenological implications of Eq. (5.7) can be explored using the methods of Ref. [32]. A preliminary estimate follows from observing that  $\mathcal{P}_L(k^2)$  is approximately equivalent to  $\mathcal{P}_S(k^2)$  if one identifies

$$b_L \sim \sqrt{M/a} = 0.57 \text{ GeV}. \quad (5.10)$$

Hence one expects that Eq. (5.7) does not generate DCSB nor confine quarks. [A value of  $b \approx 0.4 \text{ GeV} > b_c$  in  $\mathcal{P}_S(k^2)$  provides the best fit to the lattice data and this supports the same conclusion.] In order to quantitatively verify this conclusion I note that: it is the combination

$$g^2 \mathcal{P}(k^2)/k^2 \quad (5.11)$$

that appears in Eq. (2.1) and  $g^2$  is not determined in Ref. [49]; and one must extrapolate  $\mathcal{P}_L(k^2)$  outside the fitted domain. Both of these requirements are fulfilled if: 1) one assumes that a one-loop perturbative analysis is reliable for  $k^2 \gtrsim 25 \Lambda_{\text{QCD}}^2$ ; and 2) employs

$$g^2 \mathcal{P}_l(k^2) := \begin{cases} g_m^2 \mathcal{P}_L(k^2), & k^2 \leq k_m^2 \\ g^2(k^2), & k^2 > k_m^2 \end{cases}, \quad (5.12)$$

with  $g^2(k^2)$  the one-loop running coupling, requiring that  $\Delta_l(k^2) := \mathcal{P}_l(k^2)/k^2$  and its first derivative be continuous at  $k_m^2$ . This procedure yields  $\Delta_l(k^2)$  in Fig. 5 with

$$g_m = 0.65, \quad k_m^2 = 30 \Lambda_{\text{QCD}}^2. \quad (5.13)$$

It is now straightforward to solve Eq. (2.1) with a variety of *Ansätze* for the quark-gluon vertex that do not exhibit particle-like singularities. This was pursued in Ref. [48], using the methods described in Sec. 2 and renormalising at the momentum cutoff,  $\Lambda_{\text{UV}} \sim 10^4 \Lambda_{\text{QCD}}$ , for simplicity, since the  $p^2$ -evolution of  $A(p^2)$  and  $B(p^2)$  beyond that point is completely determined by

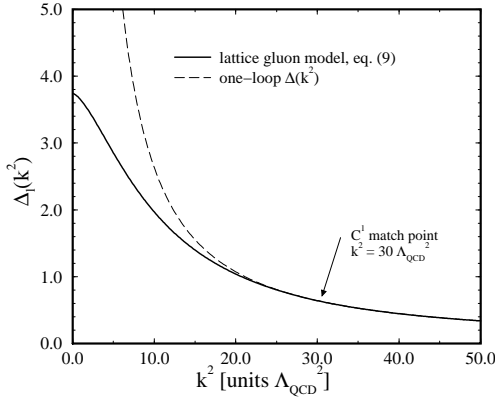


**Figure 5:**  $\Delta_l(k^2) := \mathcal{P}_l(k^2)/k^2$  from Eq. (5.12).  $\mathcal{P}_l(k^2)$  is Eq. (5.7) in the infrared and extrapolates this lattice model outside the domain accessible in the simulation [49,50]. (Adapted from Ref. [48].)

$g^2(k^2)$ . That study employed the bare vertex  $\Gamma_\mu(p, q) := \gamma_\mu$ ; the *Ansatz* [14]:

$$i\Gamma_\nu^{\text{BC}}(p, q) := i\Sigma_A(p^2, q^2) \gamma_\nu + (p + q)_\nu \quad (5.14) \\ \times \left[ \frac{1}{2} i\gamma \cdot (p + q) \Delta_A(p^2, q^2) + \Delta_B(p^2, q^2) \right],$$

where

$$\Sigma_A(p^2, q^2) := [A(p^2) + A(q^2)]/2, \\ \Delta_A(p^2, q^2) := [A(p^2) - A(q^2)]/[p^2 - q^2], \\ \Delta_B(p^2, q^2) := [B(p^2) - B(q^2)]/[p^2 - q^2]; \quad (5.15)$$

and an augmented form [8]

$$\Gamma_\mu^{\text{CP}}(p, q) := \Gamma_\mu^{\text{BC}}(p, q) + \Gamma_\mu^6(p, q), \quad (5.16)$$

$$\Gamma_\mu^6(p, q) := [\gamma_\mu(p^2 - q^2) \\ - (p + q)_\mu(\gamma \cdot p - \gamma \cdot q)] \frac{A(p^2) - A(q^2)}{2d(p, q)}, \quad (5.17)$$

with

$$d(p, q) := \frac{[p^2 - q^2]^2 + [M(p^2)^2 + M(q^2)^2]^2}{p^2 + q^2}, \quad (5.18)$$

each of which allows the quark DSE to be solved in isolation; i.e., without coupling to other DSEs. In all cases the lattice result, Eq. (5.12), yields  $M(p^2) \equiv 0$  in the chiral limit; i.e., no DCSB.

The absence of DCSB means it is straightforward to decide whether (5.12) generates confinement. Following Sec. 4, confinement is manifest

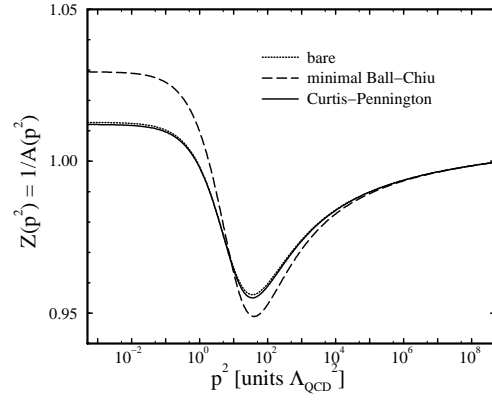


**Figure 6:**  $Z(p^2)$  obtained as the solution of Eq. (2.1) using Eq. (5.12) with: Eq. (5.14) - solid line; Eq. (5.16) - dashed line; and  $\Gamma_\mu(p, q) = \gamma_\mu$  - dotted line. That Eq. (5.7) does not confine quarks is manifest in the result:  $Z(p^2 = 0) \neq 0$ , which is independent of the vertex *Ansatz*. (Adapted from Ref. [48].)

if, for  $p^2 \simeq 0$ ,

$$Z(p^2) \propto (p^2)^\alpha, \quad \alpha \geq 1, \quad (5.19)$$

in which case the dressed-quark propagator does not have a Lehmann representation; i.e., violates the axiom of reflection positivity. The solution obtained with the vertex *Ansätze* introduced above is depicted in Fig. 6: the behaviour is qualitatively equivalent in each case and demonstrates explicitly that Eq. (5.7) does not generate confinement.

These failures: the absence of both DCSB and confinement, confirm the preliminary hypothesis based on the correspondence with  $\mathcal{P}_S$  via an effective value of  $b$ , Eq. (5.10). [The same conclusion applies to the result in Ref. [50], which is pointwise smaller in magnitude ( $\lesssim 1/3$ ) than Eq. (5.7) on the entire fitted domain.]

Equation (2.1) was also solved for  $Z(p^2)$  using

$$\tilde{\mathcal{P}}_l(k^2) := \left(1 + \varsigma e^{-k^2/\Lambda_{\text{QCD}}^2}\right) \mathcal{P}_l(k^2) \quad (5.20)$$

where  $\varsigma$  is a variable “strength” parameter. Increasing  $\varsigma$  moves the peak in  $\tilde{\mathcal{P}}_l(k^2)$  toward  $k^2 = 0$  and increases its height, thereby making it increasingly like the model of Eq. (3.9). The form of  $Z(p^2)$  is qualitatively unchanged and hence

there is no signal for the onset of confinement until  $\varsigma \gtrsim 300$ . At  $\varsigma = 300$  the maximum value is

$$\tilde{\mathcal{P}}_l(k^2 = 0.98 \Lambda_{\text{QCD}}^2) = 210 \quad (5.21)$$

and

$$\begin{aligned} \tilde{\mathcal{P}}_l(0.98 \Lambda_{\text{QCD}}^2) / \tilde{\mathcal{P}}_l(30 \Lambda_{\text{QCD}}^2) &= 16.0, \\ \text{cf. } \mathcal{P}_l(21 \Lambda_{\text{QCD}}^2) / \mathcal{P}_l(30 \Lambda_{\text{QCD}}^2) &= 1.0. \end{aligned} \quad (5.22)$$

The model of Eq. (3.9) exhibits a peak at  $k^2 = 3.7 \Lambda_{\text{QCD}}^2$  and the value of the ratio introduced above is 44, neglecting only for the purpose of this comparison the purely long-range,  $\delta^4(k)$ -part of that interaction. A comparison of

$$g_m^2 \tilde{\mathcal{P}}_l(\Lambda_{\text{QCD}}^2) \approx 89 \quad (5.23)$$

with the critical coupling of  $g_c^2 \approx 11$  in Refs. [24] shows that such large values of  $\varsigma$  ensure DCSB.

To recapitulate: in this section we have seen that in the absence of particle-like singularities in the dressed-quark-gluon vertex, extant proposals for the dressed-gluon propagator that satisfy Eq. (5.9) neither confine quarks nor break chiral symmetry dynamically. This class includes all existing estimates of  $\mathcal{P}(k^2)$  via numerical simulations.

### 5.1 Critical Interaction Tension

Furthermore the calculations described in this section reaffirm the long-standing DSE result [24] that the existence of DCSB in QCD places a constraint on the minimum phenomenologically acceptable value of the “interaction tension:”

$$\sigma^\Delta := \frac{1}{4\pi} \int_{\Lambda_{\text{QCD}}^2}^{\Lambda_{\text{pQCD}}^2} dk^2 k^2 \Theta(k^2), \quad (5.24)$$

$$\Theta(k^2) := g^2 \Delta(k^2) - g^2 \Delta(\Lambda_{\text{pQCD}}^2). \quad (5.25)$$

The lower cutoff is  $\Lambda_{\text{QCD}}$  because string-breaking becomes effective for lengths  $\gtrsim 1/\Lambda_{\text{QCD}} \sim 1$  fm, while the upper cutoff,  $\Lambda_{\text{pQCD}} = 2$  GeV, marks the boundary above which the interaction is calculable in perturbation theory. [NB. If a mechanism can be found by which singularities in the dressed-quark-gluon vertex become phenomenologically tenable then this constraint persists with the only change being  $g^2 \Delta(k^2) \rightarrow \mathcal{G}(k^2)/k^2$ ; i.e., the effective interaction.]

The lattice result, Eq. (5.12), yields

$$\sigma_l^\Delta \simeq 0.35 \text{ GeV}^2 \sim 6 \Lambda_{\text{QCD}}^2, \quad (5.26)$$

while from Ref. [32] I estimate the critical value for DCSB to be:

$$\sigma^\Delta > \sigma_c^\Delta \sim 0.5 \text{ GeV}^2 \sim 9 \Lambda_{\text{QCD}}^2, \quad (5.27)$$

with the exact value depending a little [ $\sim 20\%$ ] on model details. This is the critical value, which only supports an incipient quark condensate; i.e.,  $\langle \bar{q}q \rangle$  infinitesimally-greater-than zero. For agreement with its phenomenological value one requires [18]:

$$\sigma_{\text{phen.}}^\Delta \sim 4 \text{ GeV}^2 \sim 70 \Lambda_{\text{QCD}}^2; \quad (5.28)$$

i.e., on order-of-magnitude larger.

One additional observation: following Refs. [6,51], an estimate of the gluon condensate can be obtained from

$$\langle \alpha G G \rangle := \frac{3}{4\pi^3} \int_{\Lambda_{\text{QCD}}^2}^{\Lambda_{\text{pQCD}}^2} dk^2 k^4 \Theta(k^2). \quad (5.29)$$

The lattice model, Eq. (5.12), yields  $0.09 \text{ GeV}^4$ ; the critical value for DCSB is  $\approx 0.12 \text{ GeV}^4$ ; and the model of Ref. [18] yields  $0.42 \text{ GeV}^4$ . Contemporary analyses of QCD Sum Rules employ a value [27]:  $0.095 \pm 0.05 \text{ GeV}^4$ . However, this cannot be directly compared with the calculated values reported here because of the ambiguity in subtracting the “perturbative contribution” to the gluon correlator. Equations (5.24) - (5.29), with a subtraction that is constant below  $k^2 = \Lambda_{\text{pQCD}}^2$ , employ just one of many possibilities. Nevertheless the calculated results indicate the relevant scales.

## 6. Gluon DSE

Plainly now it is a model-independent result that DCSB requires a significant infrared enhancement in the kernel of QCD’s gap equation. Such an enhancement can also yield confinement, by ensuring that coloured  $n$ -point Schwinger functions violate reflection positivity, as discussed in Sec. 4. The question that naturally arises is: “Where does this enhancement come from?” Some guidance may be sought in studies of the DSE satisfied by the dressed-gluon propagator, which is

depicted in Fig. 4. However, as I now describe, these studies are inconclusive.

Early analyses [52] used the ghost-free axial gauge:  $n \cdot A^a = 0$ ,  $n^2 > 1$ , in which case the second equation in Fig. 4 is absent and two independent scalar functions:  $F_1$ ,  $F_2$ , are required to fully specify the dressed-gluon propagator, cf. the covariant gauge expression in Eq. (2.17), which requires only one function. In the absence of interactions:  $F_1(k^2) = -1/k^2$ ,  $F_2(k^2) \equiv 0$ . These studies employed an *Ansatz* for the three-gluon vertex that doesn't possess a particle-like singularity and neglected the coupling to the quark DSE. They also assumed  $F_2 \equiv 0$ , even nonperturbatively, and ignored it in solving the DSE. The analysis then yielded

$$F_1(k^2) \stackrel{k^2 \rightarrow 0}{\sim} \frac{1}{k^4}; \quad (6.1)$$

i.e., a marked infrared enhancement that can yield an area law for the Wilson loop [53] and hence confinement, and DCSB as described above, *without* fine-tuning.

This effect is driven by the gluon vacuum polarisation, diagram three in the first line of Fig. 4. A similar result was obtained in Ref. [54]. However, a possible flaw in these analyses was identified in Ref. [55], which argued from properties of the spectral density in ghost-free gauges that  $F_2$  cannot be zero but acts to cancel the enhancement in  $F_1$ . [NB. Retaining  $F_2$  in the analysis yields a coupled system of equations for the gluon propagator that is at least as complicated as that obtained in covariant gauges, which perhaps outweighs the apparent benefit of eliminating ghost fields in the first place.]

There have also been analyses of the gluon DSE using Landau gauge and those of Refs. [56,57] are unanimous in arriving at the covariant gauge analogue of Eq. (6.1), again driven by the gluon vacuum polarisation diagram. In these studies *Ansätze* were used for the dressed-three-gluon vertex, all of which were free of particle-like singularities. However, these studies too have weaknesses: based on an anticipated dominance of the gluon-vacuum polarisation, truncations were implemented so that only the third and fifth diagrams on the r.h.s. of the first equation in Fig. 4 were retained. In covariant gauges there is

*a priori* no reason to neglect the ghost loop contribution, diagram six, although perturbatively its contribution was estimated to be small [57].

As described on page 14, the Landau gauge studies of Refs. [34] yield a qualitatively different result: Eq. (5.5), but the question of how the particle-like singularities in the associated vertex *Ansätze* can be made consistent with the absence of coloured bound states in the strong interaction spectrum is currently unanswered. Nonetheless proponents of the result in Eq. (5.5) claim support from studies [58,59] of “complete” gauge fixing; i.e., in the outcome of attempts to construct a Faddeev-Popov-like determinant that eliminates Gribov copies or ensures that the functional integration domain for the gauge field is restricted to a subspace without them. Fixing a so-called “minimal Landau gauge,” which enforces a constraint of integrating only over gauge field configurations inside the Gribov horizon; i.e., on the simplest domain for which the Faddeev-Popov operator is invertible, the dressed-gluon 2-point function is shown to vanish at  $k^2 = 0$ . However, the approach advocated in Refs. [34] makes no use of the additional ghost-like fields necessary to restrict the integration domain. [NB. Hitherto the quantitative effect of Gribov copies in nonperturbative studies remains unknown.]

Recently the direct approach to solving the Landau gauge gluon DSE, pioneered in Refs. [56,57], has been revived by two groups:  $\mathcal{A}$ , Refs. [44,60,61]; and  $\mathcal{B}$ , Refs. [62–65], with the significant new feature that nonperturbative effects in the ghost sector are admitted; i.e., a nonperturbative solution of the DSE for the ghost propagator is sought in the form

$$G^{ab}(k) = -\delta^{ab} \frac{\varpi(k^2)}{k^2}. \quad (6.2)$$

[Without interactions,  $\varpi(k^2) \equiv 1$ .]

These studies analyse a truncated gluon-ghost DSE system, retaining only the third and sixth loop diagrams in the first equation of Fig. 4, and also the second equation. Superficially this is the same complex of equations as studied in Refs. [34]. However, the procedure for solving it is different, arguably less systematic but also less restrictive.

The difference between the groups is that  $\mathcal{A}$  employ *Ansätze* for the dressed-ghost-gluon and dressed-three-gluon vertices constructed so as to satisfy the relevant Slavnov-Taylor identities while  $\mathcal{B}$  simply use the bare vertices. Nevertheless they agree in the conclusion that in this truncation the infrared behaviour of the gluon DSE's solution is determined by the ghost loop alone: it overwhelms the gluon vacuum polarisation contribution.

That is emphasised in Ref. [64], which eliminates every loop diagram in truncating the first equation of Fig. 4 *except* the ghost loop and still recovers the behaviour of Ref. [65]. That behaviour is

$$\varpi(k^2) \sim \frac{1}{(k^2)^\kappa}, \quad d(k^2) \sim (k^2)^{2\kappa}, \quad (6.3)$$

for  $k^2 \lesssim \Lambda_{\text{QCD}}^2$ , with  $0.8 \lesssim \kappa \leq 1$ . Exact evaluation of the angular integrals that arise when solving the integral equations gives the integer-valued upper bound,  $\kappa = 1$  [63]. This corresponds to a dressed-gluon 2-point function that vanishes at  $k^2 = 0$ , although the suppression is very sudden with the propagator not peaking until  $k^2 \approx \Lambda_{\text{QCD}}^2$ , where

$$(d(k^2)/k^2)|_{k^2=\Lambda_{\text{QCD}}^2} \sim 100/\Lambda_{\text{QCD}}^2; \quad (6.4)$$

i.e., it is very much enhanced over the free propagator. [See, e.g., Ref. [44], Fig. 12.]  $\kappa = 1$  also yields a dressed-ghost propagator that exhibits a dipole enhancement analogous to that of Eq. (6.1).

A [renormalisation group invariant] running strong-coupling consistent with the truncations that yield these solutions is:

$$\alpha(k^2) := \frac{1}{4\pi} g^2 \varpi^2(k^2) d(k^2) \quad (6.5)$$

and its value at  $k^2 = 0$  is fixed by the numerical solutions:

$$\frac{\alpha(k^2=0)}{\alpha(k^2=0)} \left| \begin{array}{c|c} \mathcal{A} & \mathcal{B} \\ \hline 9.5 & \sim 4 \text{ or } 12 \end{array} \right. \quad (6.6)$$

[NB. Group  $\mathcal{A}$  approximates the angular integrals and uses vertex *Ansätze*. Group  $\mathcal{B}$  uses bare vertices and in Ref. [62] approximates the angular integrals to obtain  $\alpha(0) \sim 12$ , while in

Ref. [63] the integrals are evaluated exactly, which yields  $\alpha(0) = \frac{4}{3}\pi \approx 4.2$ .]

The qualitative feature common to both groups is that the Grassmannian ghost loops act to suppress the dressed-gluon propagator in the infrared. That may also be said of Refs. [34]. [Indications that the quark loop, diagram seven in Fig. 4, acts to oppose an enhancement of the type in Eq. (6.1) may here, with hindsight, be viewed as suggestive.]

One aspect of ghost fields is that they enter because of gauge fixing via the Fadde'ev-Popov determinant. Hence, while none of the groups introduce the additional Fadde'ev-Popov contributions advocated in Refs. [58,59], they nevertheless do admit ghost contributions, and in their solution the number of ghost fields does not have a qualitative impact. Reference [59] also obtains a dressed-propagator for the Fadde'ev-Popov fields with a  $k^2 = 0$  dipole singularity. It contributes to the action via the term employed to restrict the gauge field integration domain, in which capacity the dipole singularity can plausibly drive an area law for Wilson loops.

Schwinger functions are the primary object of study in numerical simulations of lattice-QCD and Refs. [49,50] report contemporary estimates of the lattice Landau gauge dressed-gluon 2-point function. As we saw in Sec. 5, they are consistent with a finite although not necessarily vanishing value of  $d(k^2 = 0)$ . However, simulations of the dressed-ghost 2-point function find no evidence of a dipole singularity, with the ghost propagator behaving as if  $\varpi(k^2) = 1$  in the smallest momentum bins [67]. [NB. Since the quantitative results from groups  $\mathcal{A}$  and  $\mathcal{B}$  differ and exhibit marked sensitivity to details of the numerical analysis, any agreement between the DSE results for  $\varpi(k^2)$  or  $d(k^2)$  and the lattice data on some subdomain can be regarded as fortuitous.]

The behaviour in Eqs. (6.3) also entails the presence of particle-like singularities in extant *Ansätze* for the dressed-ghost-gluon, dressed-three-gluon and dressed-quark-gluon vertices that are consistent with the relevant Slavnov-Taylor identities. [ $\kappa = 1$  corresponds to an ideal simple pole singularity.] Hence while this behaviour may be consistent with the confinement of elementary excitations, as currently elucidated it also pre-

dicts the existence of coloured bound states in the strong interaction spectrum [see page 13].

Furthermore, while it does yield a running strong-coupling with  $\alpha(k^2 = 0) \gtrsim 1$ , that, as we saw in Sec. 5, makes DCSB dependent on fine tuning. To make this plain, the maximum value of 12 in Eq. (6.6) yields  $\sigma^\Delta \approx 0.7 \text{ GeV}^2$ , which is just above  $\sigma_c^\Delta$  but falls far short of the value required to produce the physical value of the quark condensate. In fact, the quark condensate is only  $\sim 5\%$  of the phenomenologically required value in Eq. (3.30) [66]. Notwithstanding these remarks, the studies of Refs. [44,60,61] and subsequently Refs. [62–65] are laudable. They have focused attention on a previously unsuspected qualitative sensitivity to truncations in the gauge sector.

To recapitulate. It is clear from Sec. 5 that DCSB requires the effective interaction in the quark DSE to be strongly enhanced at  $k^2 \sim \Lambda_{\text{QCD}}^2$ . [Remember too that in Sec. 3, Figs. 2, we saw that modern lattice simulations confirm the pattern of behaviour exhibited by quark DSE solutions obtained with such an enhanced interaction.] Studies of QCD's gauge sector indicate that gluon-gluon and/or gluon-ghost dynamics can generate such an enhancement. However, the qualitative nature of the mechanism and its strength remains unclear: is it the gluon vacuum polarisation or that of the ghost that is the driving force? It is a contemporary challenge to explore and understand this.

## 7. Bethe-Salpeter Equation

Hitherto I have focussed on the not-directly-observable elementary excitations in QCD. They make themselves manifest in hadrons and their properties. In quantum field theory, two and three-body bound states are, respectively, described by the Poincaré-covariant Bethe-Salpeter and Fadde'ev equations. Solving an equation of this type yields the bound states mass and also an amplitude that describes the bound state constraints on the constituents' momenta. This amplitude is a valuable intuitive guide and, in cases where a simple quark model analogue of the bound state exists, the amplitude incorpo-

rates and extends the information present in that analogue's quantum mechanical wave function.

In quantum field theory, as in classical mechanics, the interacting two-body problem is much simpler than that of three such bodies, and I illustrate the bound state application of DSEs by considering mesons. The renormalised homogeneous BSE for a bound state of a dressed-quark and dressed-antiquark with total momentum  $P$  is

$$[\Gamma_H(k; P)]_{tu} = \int_q^\Lambda [\chi(q; P)]_{rs} K_{tu}^{rs}(q, k; P), \quad (7.1)$$

$$\chi_H(q; P) := \mathcal{S}(q_+) \Gamma_H(q; P) \mathcal{S}(q_-), \quad (7.2)$$

with:  $\Gamma_H(k; P)$  the Bethe-Salpeter amplitude, where  $H$  specifies the flavour structure of the meson;  $\mathcal{S}(p) := \text{diag}[S_u(p), S_d(p), S_s(p)]$ ;  $q_+ = q + \eta_P P$ ,  $q_- = q - (1 - \eta_P)P$ ; and  $r, \dots, u$  represent colour-, Dirac- and flavour-matrix indices. [ $\eta_P \in [0, 1]$  is the momentum partitioning parameter. It appears in Poincaré covariant treatments because, in general, the definition of the relative momentum is arbitrary. Physical observables, such as the mass, must be independent of  $\eta_P$  but that is only possible if the Bethe-Salpeter amplitude depends on it.  $\eta_P = 1/2$  for charge-conjugation eigenstates.]

The general form of the Bethe-Salpeter amplitude for pseudoscalar mesons is

$$\begin{aligned} \Gamma_H(k; P) = & \quad (7.3) \\ & \mathcal{T}^H \gamma_5 \left[ iE_H(k; P) + \gamma \cdot P F_H(k; P) \right. \\ & \left. + \gamma \cdot k \, k \cdot P G_H(k; P) + \sigma_{\mu\nu} k_\mu P_\nu H_H(k; P) \right], \end{aligned}$$

where for bound states of constituents with equal current-quark masses, the scalar functions  $E$ ,  $F$ ,  $G$  and  $H$  are even under  $k \cdot P \rightarrow -k \cdot P$ . [NB. Since the homogeneous BSE is an eigenvalue problem,  $E_H(k; P) = E_H(k^2, k \cdot P | P^2)$ , etc.; i.e.,  $P^2$  is not a variable, instead it labels the solution.]

In Eq. (7.1),  $K_{tu}^{rs}(q, k; P)$  is the renormalised, fully-amputated quark-antiquark scattering kernel, which also appears implicitly in Eq. (2.1) because it is the kernel of the inhomogeneous DSE satisfied by  $\Gamma_\nu(q; p)$ .  $K_{tu}^{rs}(q, k; P)$  is a 4-point Schwinger function, obtained as the sum

of a countable infinity of skeleton diagrams. It is two-particle-irreducible, with respect to the quark-antiquark pair of lines and does not contain quark-antiquark to single gauge-boson annihilation diagrams, such as would describe the leptonic decay of a pseudoscalar meson. (A connection between the fully-amputated quark-antiquark scattering amplitude:  $M = K + K(SS)K + \dots$ , and the Wilson loop is discussed in Ref. [68].)

The complexity of  $K_{tu}^{rs}(q, k; P)$  is one reason why quantitative studies of the quark DSE currently employ *Ansätze* for  $D_{\mu\nu}(k)$  and  $\Gamma_\nu(k, p)$ . However, as illustrated by Ref. [25], this complexity does not prevent one from analysing aspects of QCD in a model independent manner and proving general results that provide useful constraints on model studies. [NB. References [25, 18, 69–71] provide a pedagogical guide to the rigorous and practical application of BSEs to the light-quark sector of QCD, and should be particularly helpful to practitioners for whom their efficacy has not hitherto been apparent.]

$K$  has a skeleton expansion in terms of the elementary, dressed-particle Schwinger functions; e.g., the dressed-quark and -gluon propagators. The first two orders in one systematic expansion [3] are depicted in Figs. 7, 8. This particular expansion, in concert with its analogue for the kernel in the quark DSE, provides a means of constructing a kernel that, order-by-order in the number of vertices, ensures the preservation of vector and axial-vector Ward-Takahashi identities. This is particularly important in QCD where the Goldstone boson nature of the pion must be understood as a *consequence* of its internal structure, and without fine-tuning; i.e., the masslessness of the pion in the chiral limit cannot arise as the result of carefully varying parameters in a putative potential. The Goldstone boson character of the pion is easily understood via the interrelation between the pseudoscalar BSE and quark DSE [3, 4, 25].

Analysing the flavour-nonsinglet inhomogeneous axial-vector BSE and its pseudoscalar analogue one obtains, via the axial-vector Ward-Takahashi identity, a mass formula, exact in QCD, for pseudoscalar mesons [4, 25, 72]:

$$f_H m_H^2 = \mathcal{M}_H^\zeta r_H^\zeta, \quad (7.4)$$

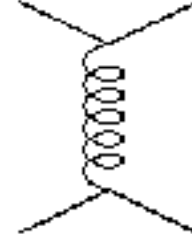


**Figure 7:** Leading [Ladder] contribution to the systematic expansion of the quark-antiquark scattering kernel introduced in Ref. [3]. In this expansion, the propagators are dressed but the vertices are bare. (Adapted from Ref. [3].)

$\mathcal{M}_H^\zeta = \text{tr}_F[M_\zeta\{\mathcal{T}^H, (\mathcal{T}^H)^\dagger\}]$ , where  $\mathcal{T}^H$  is a matrix that describes the flavour content of the meson; e.g.,  $\mathcal{T}^{\pi^+} = \frac{1}{2}(\lambda_F^1 + i\lambda_F^2)$ ,  $(\cdot)^\dagger$  denotes matrix transpose, and

$$\frac{1}{\sqrt{2}} f_H P_\mu = Z_2 \text{tr} \int_k^\Lambda (\mathcal{T}^H)^\dagger \gamma_5 \gamma_\mu \chi_H(k; P), \quad (7.5)$$

$$r_H^\zeta = -i\sqrt{2} Z_4 \text{tr} \int_k^\Lambda (\mathcal{T}^H)^\dagger \gamma_5 \chi_H(k; P) \quad (7.6)$$

$$:= -2i \langle \bar{q}q \rangle_\zeta^H \frac{1}{f_H}.$$

Importantly, the expression in Eq. (7.4) is valid for *all* values of the current-quark mass. [NB. In this section the normalisation is such that  $f_\pi = 131 \text{ MeV}$ .]

Equation (7.5) gives the formula for the residue of the meson's pole in the axial-vector vertex, which completely determines the strong interaction contribution to its leptonic decay. The factor of  $Z_2$  on the r.h.s. is just that necessary to ensure that  $f_H$  is independent of the renormalisation point, regularisation mass-scale and gauge parameter; i.e., to ensure that  $f_H$  is truly a physical observable. Its intuitive character is also plain: it is the gauge-invariant projection of the meson's Bethe-Salpeter wave function at the origin.

Equation (7.6) is the expression for the residue of the meson's pole in the pseudoscalar vertex. In this case again the factor  $Z_4$  on the r.h.s. depends on the gauge parameter, the regularisation mass-scale and the renormalisation point. This dependence is exactly that required to ensure that: 1)  $r_H$  is finite in the limit  $\Lambda \rightarrow \infty$ ; 2)

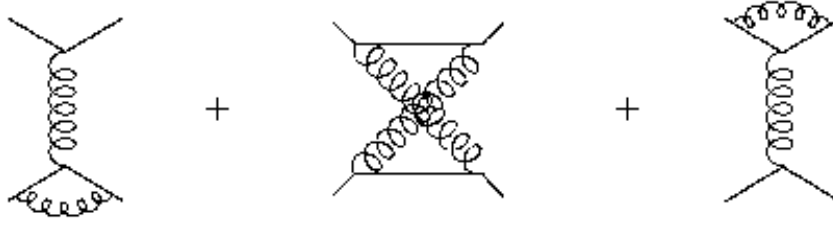


**Figure 8:** Next-to-leading order contribution in the truncation scheme of Ref. [3]. (Adapted from Ref. [3].)

$r_H$  is gauge-parameter independent; and 3) the renormalisation point dependence of  $r_H$  is just such as to ensure that the r.h.s. of Eq. (7.4) is renormalisation point *independent*.

These formulae exemplify the manner in which gauge invariant results are obtained from the gauge covariant Schwinger functions the DSEs yield.

It is straightforward to show that in the chiral limit, defined in Eq. (2.15), Eq. (7.6) yields

$$r_H^\zeta \xrightarrow{\hat{m} \rightarrow 0} = \frac{2}{f_\pi^0} \langle \bar{q}q \rangle_\zeta^0, \quad (7.7)$$

where  $\langle \bar{q}q \rangle_\zeta^0$  is the vacuum quark condensate, Eq. (3.26), and  $f_\pi^0$  is the pseudoscalar meson decay constant in the chiral limit. Hence, as a corollary of Eq. (7.4) one recovers [25] what is commonly called the ‘‘Gell-Mann–Oakes–Renner’’ relation:

$$f_H^2 m_H^2 = 4 m_\zeta \langle \bar{q}q \rangle_\zeta^0 + O(\hat{m}^2). \quad (7.8)$$

Another particularly important result is that the axial-vector Ward-Takahashi identity also constrains the chiral limit behaviour of the scalar functions in Eq. (7.3). This is a pointwise manifestation of Goldstone’s theorem with [25]:

$$\frac{1}{\sqrt{2}} f_\pi^0 E_\pi(k; 0) = B(k^2), \quad (7.9)$$

$$F_R(k; 0) + \sqrt{2} f_\pi^0 F_\pi(k; 0) = A(k^2), \quad (7.10)$$

$$G_R(k; 0) + \sqrt{2} f_\pi^0 G_\pi(k; 0) = 2A'(k^2), \quad (7.11)$$

$$H_R(k; 0) + \sqrt{2} f_\pi^0 H_\pi(k; 0) = 0. \quad (7.12)$$

In these identities  $(\cdot)_\pi$  denotes solution functions obtained in the chiral limit and  $(\cdot)_R$  are functions appearing in the pole-free part of the inhomogeneous axial-vector vertex.

The formula in Eq. (7.9) is a quark-level Goldberger-Treiman relation, exact in QCD, while the next two identities indicate that pseudoscalar mesons necessarily have a pseudovector component.

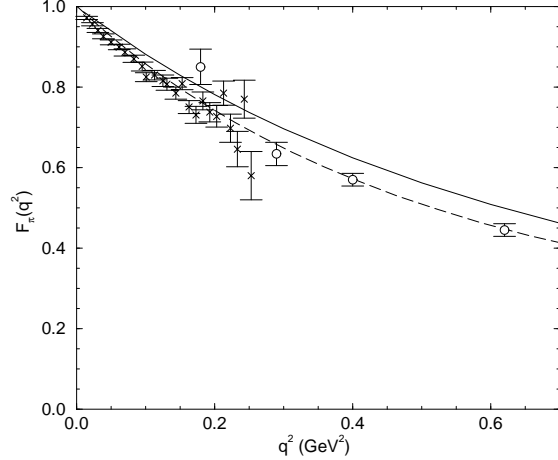


**Figure 9:** Small- $q^2$  pion form factor calculated in Ref. [73] and compared with data from Refs. [75] (circles) and [76] (crosses). The solid line is the result obtained including the pseudovector components while the dashed line was obtained without them [74]. Clearly they contribute little on this domain. (Adapted from Ref. [73].)

This is crucial because it is these amplitudes that dominate the mesons’ electromagnetic form factors at large meson energy and yield [73]

$$q^2 F_H(q^2) = \text{constant at large-}q^2, \quad (7.13)$$

up to logarithmic corrections, making a connection with the result of perturbative QCD analyses. If the pseudovector amplitudes are ignored one finds instead [74] that  $(q^2)^2 F_H(q^2) = \text{constant at large-}q^2$ . These results are illustrated in Figs. 9, 10. They are, of course, contingent upon Eq. (3.25), which describes the correct ultraviolet behaviour of the mass function in QCD. Any model that employs/predicts a mass function that falls faster than a single power of  $1/p^2$  will be in conflict with perturbative analyses of

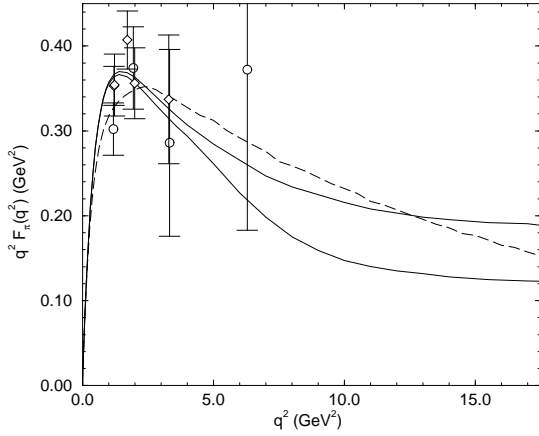


**Figure 10:** Calculated [73] form factor compared with the largest  $q^2$  data available: diamonds - Ref. [75]; and circles - Ref. [77]. The solid lines are the results obtained when the pseudovector components of the pion Bethe-Salpeter amplitude are included (two limiting models were employed in the calculation), the dashed-line when they are neglected [74]. On this domain the difference is plain, with only the solid lines exhibiting Eq. (7.13). (Adapted from Ref. [73].)

the form factors. [NB. No bound state amplitude can fall slower than  $1/p^2$ .]

### 7.1 Heavy-quark Limit

After this focus on the light-quark sector I now return to Eqs. (7.4)–(7.6) and note that they also have two important corollaries valid in the limit of large current-quark mass. To elucidate them one rewrites the total momentum

$$P_\mu = m_H v_\mu = (\hat{M}_Q + E_H), \quad (7.14)$$

where:  $m_H$  is the heavy-hadron's mass;  $\hat{M}_Q$  is a constituent-heavy-quark mass,  $\hat{M}_Q \approx M_Q^E \approx \hat{m}_Q$  for heavy-quarks, as illustrated in Fig. 1; and  $E_H$  is the “binding energy.”

Now the dressed propagator for the heavy-quark in the heavy-meson can be written [30]

$$S_Q(k+P) = \frac{1}{2} \frac{1 - i\gamma \cdot v}{k \cdot v - E_H} + \mathcal{O}\left(\frac{|k|}{\hat{M}_Q}, \frac{E_H}{\hat{M}_Q}\right), \quad (7.15)$$

where  $k$  is the momentum of the lighter constituent, and the canonically normalised Bethe-Salpeter amplitude can be expressed as

$$\Gamma_H(k; P) = \sqrt{m_H} \Gamma_H^{<\infty}(k; P) \quad (7.16)$$

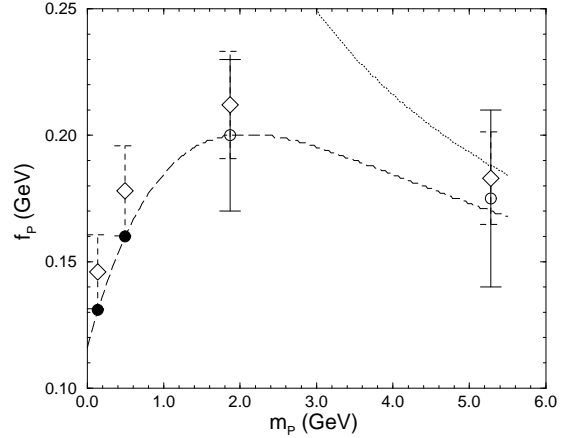


**Figure 11:** Mass-dependence of the meson leptonic decay constant. Experimental values of  $f_{\pi,K}$ , filled circles; lattice estimates [79] of  $f_D = 0.20 \pm 0.03$  GeV and  $f_B = 0.17 \pm 0.035$  GeV, open circles; decay constants calculated in Ref. [22] with an estimated 10% theoretical error. The dashed line is an eye-guiding fit to the experimental and lattice estimates, which exhibits the large- $m_H$  limit of Eq. (7.17). The dotted line is the large- $m_H$  limit of this fit. (Adapted from Ref. [22].)

where  $\Gamma_H^{<\infty}(k; P)$  is pointwise-finite in the limit  $m_H \rightarrow \infty$ . It is obvious that in the calculation of observables the meson's Bethe-Salpeter amplitude will limit the range of  $|k|$  so that Eq. (7.15) will be a good approximation if-and-only-if both the momentum space width of the amplitude and the binding energy are significantly less-than  $\hat{M}_Q$ .

Using Eqs. (7.15) and (7.16) in Eq. (7.5) yields

$$f_H = \frac{c_H^f}{\sqrt{m_H}}, \quad (7.17)$$

where  $c_H^f$  is a calculable and finite constant that depends only on  $\Gamma_H^{<\infty}(k; P)$  and the dressed-light-quark propagator. In Eq. (7.17) the DSEs reproduce a well-known general consequence of heavy-quark symmetry. Since  $f_\pi < f_K$  is an experimental fact neither this formula nor the limits that lead to it are valid for light mesons. The actual situation, as determined in Ref. [22], is depicted in Fig. 11. Clearly, finite current-quark mass corrections are significant for the  $c$ -quark. In fact, such corrections can be  $\lesssim 30\%$  in  $b \rightarrow c$  transitions and as much as a factor of two in  $c \rightarrow d$

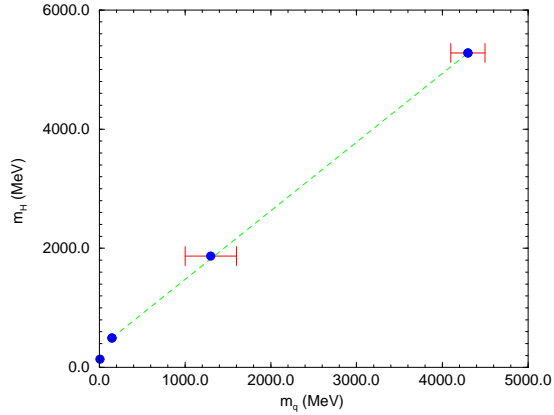


**Figure 12:** Mass-dependence of meson masses. Experimental value of the masses and estimates of  $m_q$ , are taken from Ref. [17]. The straight line, drawn through the  $D$ - and  $B$ -meson masses, depicts the linear trajectory predicted in Eq. (7.19). (Adapted from Ref. [78].)

transitions [22].

Applying the same analysis to Eq. (7.6) gives

$$r_H = c_H^{r\zeta} \sqrt{m_H}, \quad (7.18)$$

where again  $c_H^{r\zeta}$  is a calculable and finite constant. Using this and Eq. (7.17) in Eq. (7.4) one finds [22,78] that in the heavy-quark limit

$$m_H = \frac{c_H^{r\zeta}}{c_H^f} \mathcal{M}_H^\zeta. \quad (7.19)$$

Thus the quadratic trajectory of Eq. (7.8) evolves into a linear trajectory when the current-quark mass becomes large; i.e., the mass of a heavy-meson rises linearly with the mass of its heaviest constituent. This is illustrated in Fig. 12, which indicates that a linear trajectory may describe all but the  $\pi$ -meson. That was anticipated in Ref. [4] and later clarified in an explicit calculation [21] where the onset of the linear trajectory was observed at 2–3-times the  $s$ -quark current-mass.

Explicit calculations, of course, require that the form of the scattering kernel be specified. The dressed-ladder form

$$K_{tu}^{rs}(q, k; P) = \mathcal{G}(k^2) D_{\mu\nu}^{\text{free}}(p - q) \left[ \frac{1}{2} \lambda^a \gamma_\mu \right]_{tr} \left[ \frac{1}{2} \lambda^a \gamma_\nu \right]_{su}, \quad (7.20)$$

in concert with Eq. (3.9) in the quark DSE, ensures that the vector and axial-vector Ward-Ta-

kahashi identities are satisfied. Preserving these identities is important because it guarantees current conservation in electromagnetic processes and an explicit realisation of the consequences of DCSB as elucidated herein. The choice in Eq. (7.20) is that yielded by the truncation scheme of Ref. [3] and clearly maintains the ultraviolet behaviour of QCD, Eq. (3.5).

With an explicit form for the kernel, Eq. (7.1) is an eigenvalue problem and it has solutions only for particular, separated values of  $P^2$ . The eigenvector associated with each eigenvalue:  $\Gamma_H(k; P)$ , the Bethe-Salpeter amplitude, is a one-particle-irreducible, fully-amputated quark-meson vertex. In the flavour non-singlet pseudoscalar channels the solutions having the lowest eigenvalues correspond to the  $\pi$ - and  $K$ -mesons, while in the vector channels they correspond to the  $\omega$ -,  $\rho$ - and  $\phi$ -mesons.

To calculate meson masses, one first solves Eqs. (3.14) and (3.15) for the renormalised dressed-quark propagator. This numerical solution for  $S(p)$  is then used in the BSE [obtained using Eqs. (7.1), (7.3), (7.20)], which for pseudoscalar mesons is a coupled set of four homogeneous equations, one set for each meson. Solving the equations is a challenging numerical exercise, requiring careful attention to detail, and two complementary methods were both used in Refs. [4,18]. While the numerical methods were identical, the authors of Ref. [18] used a simplified version of the effective interaction:

$$\frac{\mathcal{G}(k^2)}{k^2} = \frac{4\pi^2}{\omega^6} D k^2 e^{-k^2/\omega^2} + 4\pi \frac{\gamma_{m\pi}}{\frac{1}{2} \ln \left[ \tau + \left( 1 + k^2/\Lambda_{\text{QCD}}^2 \right)^2 \right]} \mathcal{F}(k^2), \quad (7.21)$$

and varied the single parameter  $D$  along with the current-quark masses:  $\hat{m}_u = \hat{m}_d$  and  $\hat{m}_s$ , in order to reproduce the observed values of  $m_\pi$ ,  $m_K$  and  $f_\pi$  listed on page 3. The many other calculated results in Refs. [18,69,70] are *predictions* in the sense that they are unconstrained. A particular feature of these studies is that the Poincaré covariant four-dimensional BSE is solved directly eschewing the commonly used artifice of a three-dimensional reduction, which introduces spurious effects when imposing compatibility with

Goldstone's theorem and can also lead to the misinterpretation of a model's parameters [80].

## 8. Epilogue

I have focused on some robust qualitative aspects of Dyson-Schwinger equation [DSE] studies. A compelling complement is Ref. [71], which describes in detail the direct application of the single-parameter DSE-model of Eq. (7.21) to the spectrum and dynamical properties of light mesons. Additional important aspects are described in Ref. [81]: in particular the use of vector meson polarisation observables to probe the long-range part of the quark-quark interaction, which highlights the intuitive character of Bethe-Salpeter amplitudes; and also in Refs. [73,74,82] where the manner in which the DSEs provide for the intrinsic preservation of current-algebra's anomalies is elucidated and exemplified. Light-baryon properties too have been studied, with Ref. [83] demonstrating that a quark-diquark simplification [84] of the covariant baryon Fadde'ev equation is a good foundation for spectroscopy, and Refs. [85] proving it efficacious for a wide range of scattering observables.

In recent years there has also been a renewal of interest in DSE applications to QCD at non-zero chemical potential and temperature, which herein I have not mentioned at all. In closing therefore I note that, as will have become clear from Secs. 3 and 4, confinement and dynamical chiral symmetry breaking are simultaneously accessible using the DSEs. This was exploited in Ref. [86] wherein a well-constrained DSE-model of QCD was used to explore the deconfinement and chiral symmetry restoration transitions at  $T \neq 0$ : in this case the transitions are coincident and second order, which is easily understood via the causal relation between these two phenomena and the behaviour of the dressed-quark mass function.

More recently the nonzero temperature and density applications have expanded to include hadron properties, as illustrated in Refs. [87], and have become more refined. A large part of Ref. [1] is a chronicle of this. Reference [1] also highlights a contemporary challenge in this area: the development of a DSE-based quantum trans-

port theory. That quest is driven by a desire to incorporate the treatment of out-of-equilibrium aspects of a relativistic heavy ion collision into a framework that reliably describes the chemical and thermal equilibrium features of hot and dense strongly-interacting matter.

**Acknowledgments.** I am grateful for the hospitality and support of the Erwin Schrödinger Institute for Mathematical Physics, Vienna, during my two engagements at this workshop, and observe that it is indeed true that kangaroos are rare in Australia. In preparing this contribution I have drawn heavily on research completed in collaboration with F.T. Hawes, M.A. Ivanov, Yu.L. Kalinovsky, P. Maris, S.M. Schmidt and P.C. Tandy. This work was supported by the US Department of Energy, Nuclear Physics Division, under contract no. W-31-109-ENG-38.

## A. Euclidean Metric Conventions

For 4-vectors  $a, b$ :

$$a \cdot b := a_\mu b_\nu \delta_{\mu\nu} := \sum_{i=1}^4 a_i b_i, \quad (\text{A.1})$$

so that a spacelike vector,  $Q_\mu$ , has  $Q^2 > 0$ . The Dirac matrices are Hermitian and defined by the algebra

$$\{\gamma_\mu, \gamma_\nu\} = 2\delta_{\mu\nu}; \quad (\text{A.2})$$

and

$$\gamma_5 := -\gamma_1\gamma_2\gamma_3\gamma_4 \quad (\text{A.3})$$

so that

$$\text{tr} [\gamma_5 \gamma_\mu \gamma_\nu \gamma_\rho \gamma_\sigma] = -4 \varepsilon_{\mu\nu\rho\sigma}, \quad \varepsilon_{1234} = 1. \quad (\text{A.4})$$

The Dirac-like representation of these matrices is:

$$\vec{\gamma} = \begin{pmatrix} 0 & -i\vec{\tau} \\ i\vec{\tau} & 0 \end{pmatrix}, \quad \gamma_4 = \begin{pmatrix} \tau^0 & 0 \\ 0 & -\tau^0 \end{pmatrix}, \quad (\text{A.5})$$

where the  $2 \times 2$  Pauli matrices are:

$$\begin{aligned} \tau^0 &= \begin{pmatrix} 1 & 0 \\ 0 & 1 \end{pmatrix}, & \tau^1 &= \begin{pmatrix} 0 & 1 \\ 1 & 0 \end{pmatrix}, \\ \tau^2 &= \begin{pmatrix} 0 & -i \\ i & 0 \end{pmatrix}, & \tau^3 &= \begin{pmatrix} 1 & 0 \\ 0 & -1 \end{pmatrix}. \end{aligned} \quad (\text{A.6})$$

## References

- [1] C.D. Roberts and S.M. Schmidt, “Dyson-Schwinger Equations: Density, Temperature and Continuum Strong QCD,” to appear in *Prog. Part. Nucl. Phys.* **45** (2000).
- [2] C.D. Roberts and A.G. Williams, *Prog. Part. Nucl. Phys.* **33** (1994) 477.
- [3] A. Bender, C.D. Roberts and L. v. Smekal, *Phys. Lett. B* **380** (1996) 7.
- [4] P. Maris and C. D. Roberts, *Phys. Rev. C* **56**, 3369 (1997).
- [5] A.W. Schreiber, T. Sizer and A.G. Williams, “Dimensionally regularized study of nonperturbative quenched QED,” in *Proc. of the Workshop on Nonperturbative Methods in Quantum Field Theory*, edited by A.W. Schreiber, A.G. Williams and A.W. Thomas (World Scientific, Singapore, 1998) pp. 299-307.
- [6] G. Krein, C.D. Roberts and A.G. Williams, *Int. J. Mod. Phys. A* **7** (1992) 5607.
- [7] M. Reenders, Dynamical symmetry breaking in the gauged Nambu-Jona-Lasinio model, PhD Thesis, University of Groningen (1999); M. Reenders, “On the nontriviality of Abelian gauged Nambu-Jona-Lasinio models in four dimensions,” hep-th/9908158; and references therein.
- [8] D. C. Curtis and M.R. Pennington, *Phys. Rev. D* **42** (1990) 4165.
- [9] Z. Dong, H.J. Munczek and C.D. Roberts, *Phys. Lett. B* **333** (1994) 536; A. Bashir, A. Kizilersu and M.R. Pennington, *Phys. Rev. D* **57** (1998) 1242.
- [10] A. Bashir, A. Kizilersu and M.R. Pennington, “Analytic form of the one-loop vertex and of the two-loop fermion propagator in 3-dimensional massless QED,” hep-ph/9907418.
- [11] F.T. Hawes and A.G. Williams, *Phys. Lett. B* **268** (1991) 271; F. T. Hawes, *Fermion Dyson-Schwinger studies in QED and QCD: Comparisons of ansatz for boson propagator and vertex*, PhD Thesis, Florida State University (1994).
- [12] M.R. Pennington, “Mass production requires precision engineering,” in *Proc. of the Workshop on Nonperturbative Methods in Quantum Field Theory*, edited by A.W. Schreiber, A.G. Williams and A.W. Thomas (World Scientific, Singapore, 1998) pp. 49-60; A. Bashir and M.R. Pennington, *Phys. Rev. D* **50** (1994) 7679.
- [13] P. Pascual and R. Tarrach, *QCD: Renormalization For The Practitioner* (Springer-Verlag, Berlin, 1984).
- [14] J. S. Ball and T.-W. Chiu, *Phys. Rev. D* **22** (1980) 2542.
- [15] See also: S. K. Kim and M. Baker, *Nucl. Phys. B* **164** (1980) 152; and J. S. Ball and T.-W. Chiu, *Phys. Rev. D* **22** (1980) 2550.
- [16] H.J. Munczek and A.M. Nemirovsky, *Phys. Rev. D* **28** (1983) 181.
- [17] C. Caso *et al.*, *Eur. Phys. J. C* **3** (1998) 1.
- [18] P. Maris and P.C. Tandy, *Phys. Rev. C* **60** (1999) 055214.
- [19] R. Fukuda and T. Kugo, *Nucl. Phys. B* **117** (1976) 250; C.D. Roberts and R.T. Cahill, *Phys. Rev. D* **33** (1986) 1755.
- [20] S. Capstick and B.D. Keister, “Baryon magnetic moments in a relativistic quark model,” nucl-th/9611055.
- [21] P. Maris and C.D. Roberts, “Differences between heavy and light quarks,” in *Proc. of the IVth International Workshop on Progress in Heavy Quark Physics*, edited by M. Beyer, T. Mannel and H. Schröder (University of Rostock, Rostock, 1998) pp. 159-162.
- [22] M.A. Ivanov, Yu.L. Kalinovsky and C.D. Roberts, *Phys. Rev. D* **60** (1999) 034018.
- [23] K. Lane, *Phys. Rev.* **10** (1974) 2605; H. D. Politzer, *Nucl. Phys. B* **117** (1976) 397.
- [24] K. Higashijima, *Phys. Rev. D* **29** (1984) 1228; D. Atkinson and P.W. Johnson, *Phys. Rev. D* **37** (1988) 2296; C.D. Roberts and B.H. McKellar, *Phys. Rev. D* **41** (1990) 672; A.G. Williams, G.Krein and C.D. Roberts, *Annals Phys.* **210** (1991) 464.
- [25] P. Maris, C.D. Roberts and P.C. Tandy, *Phys. Lett. B* **420** (1998) 267.
- [26] D.I. Diakonov and V.Y. Petrov, *Nucl. Phys. B* **272** (1986) 457.
- [27] D.B. Leinweber, *Annals Phys.* **254** (1997) 328.
- [28] J.I. Skullerud and A.G. Williams, “Quark propagator in Landau gauge,” hep-lat/0007028; and A.G. Williams, these proceedings.
- [29] J.C.R. Bloch, C.D. Roberts and S.M. Schmidt, *Phys. Rev. C* **61** (2000) 065207.
- [30] M.A. Ivanov, Yu.L. Kalinovsky, P. Maris and C.D. Roberts, *Phys. Lett. B* **416** (1998) 29.

- [31] J. Glimm and A. Jaffee, *Quantum Physics. A Functional Point of View* (Springer-Verlag, New York, 1981).
- [32] F.T. Hawes, C.D. Roberts and A.G. Williams, *Phys. Rev. D* **49** (1994) 4683.
- [33] L.C.L. Hollenberg, C.D. Roberts and B.H.J. McKellar, *Phys. Rev. C* **46** (1992) 2057.
- [34] U. Häbel, R. Könnig, H.G. Reusch, M. Stingl and S. Wigard, *Z. Phys. A* **336** (1990) 423; *ibid* 435; M. Stingl, *Z. Phys. A* **353** (1996) 423.
- [35] P. Maris, *Phys. Rev. D* **52** (1995) 6087.
- [36] M. Göpfert and G. Mack, *Commun. Math. Phys.* **82** (1981) 545.
- [37] T.W. Appelquist, M. Bowick, D. Karabali and L.C. Wijewardhana, *Phys. Rev. D* **33** (1986) 3704.
- [38] C.J. Burden and C.D. Roberts, *Phys. Rev. D* **44** (1991) 540.
- [39] C.J. Burden, J. Praschifka and C.D. Roberts, *Phys. Rev. D* **46** (1992) 2695.
- [40] M.B. Einhorn, *Phys. Rev. D* **14** (1976) 3451.
- [41] R.F. Streater and A.S. Wightman, *PCT, Spin and Statistics*, 3rd edition (Addison-Wesley, Reading, Mass., 1980).
- [42] P. Bicudo, N. Brambilla, E. Ribeiro and A. Vairo, *Phys. Lett. B* **442** (1998) 349; F.J. Llanes-Estrada and S.R. Cotanch, *Phys. Rev. Lett.* **84** (2000) 1102.
- [43] C. Parrinello, *Phys. Rev. D* **50** (1994) R4247.
- [44] L. v. Smekal, A. Hauck and R. Alkofer, *Annals Phys.* **267** (1998) 1.
- [45] J. Papavassiliou and J.M. Cornwall, *Phys. Rev. D* **44** (1991) 1285.
- [46] A. Bender and R. Alkofer, *Phys. Rev. D* **53** (1996) 446.
- [47] A.A. Natale and P.S. Rodrigues da Silva, *Phys. Lett. B* **392** (1997) 444.
- [48] F.T. Hawes, P. Maris and C.D. Roberts, *Phys. Lett. B* **440** (1998) 353.
- [49] P. Marenzoni, G. Martinelli and N. Stella, *Nucl. Phys. B* **455** (1995) 339;
- [50] D.B. Leinweber, J.I. Skullerud, A.G. Williams and C. Parrinello [UKQCD Collaboration], *Phys. Rev. D* **60** (1999) 094507.
- [51] H.B. Tang and R.J. Furnstahl, "The Gluon condensate and running coupling of QCD," hep-ph/9502326.
- [52] M. Baker, J.S. Ball and F. Zachariasen, *Nucl. Phys. B* **186** (1981) 531; *ibid* 560.
- [53] G.B. West, *Phys. Lett. B* **115** (1982) 468.
- [54] D. Atkinson, P.W. Johnson, W.J. Schoenmaker and H.A. Slim, *Nuovo Cim.* **77 A** (1983) 197.
- [55] G.B. West, *Phys. Rev. D* **27** (1983) 1878.
- [56] S. Mandelstam, *Phys. Rev. D* **20** (1979) 3223; U. Bar-Gadda, *Nucl. Phys. B* **163** (1980) 312; N. Brown and M.R. Pennington, *Phys. Lett. B* **202** (1988) 257; N. Brown and M.R. Pennington, *Phys. Rev. D* **38** (1988) 2266.
- [57] N. Brown and M.R. Pennington, *Phys. Rev. D* **39** (1989) 2723.
- [58] D. Zwanziger, *Nucl. Phys. B* **364** (1991) 127.
- [59] D. Zwanziger, *Nucl. Phys. B* **412** (1994) 657.
- [60] L. v. Smekal, R. Alkofer and A. Hauck, *Phys. Rev. Lett.* **79** (1997) 3591.
- [61] A. Hauck, R. Alkofer and L. v. Smekal, "A solution to coupled Dyson-Schwinger equations for gluons and ghosts in Landau gauge," in *Proc. of the Workshop on Nonperturbative Methods in Quantum Field Theory*, edited by A.W. Schreiber, A.G. Williams and A.W. Thomas (World Scientific, Singapore, 1998) pp. 81-89.
- [62] D. Atkinson and J.C.R. Bloch, *Phys. Rev. D* **58** (1998) 094036.
- [63] D. Atkinson and J.C.R. Bloch, *Mod. Phys. Lett. A* **13** (1998) 1055.
- [64] D. Atkinson, "Infrared and ultraviolet coupling in QCD," in *Proc. of the Workshop on Nonperturbative Methods in Quantum Field Theory*, edited by A.W. Schreiber, A.G. Williams and A.W. Thomas (World Scientific, Singapore, 1998) pp. 69-80.
- [65] J.C.R. Bloch, "Infrared fixed point of the running coupling in QCD," in *Proc. of the Workshop on Nonperturbative Methods in Quantum Field Theory*, edited by A.W. Schreiber, A.G. Williams and A.W. Thomas (World Scientific, Singapore, 1998) pp. 90-96.
- [66] J.C.R. Bloch, unpublished.
- [67] H. Suman and K. Schilling, *Phys. Lett. B* **373** (1996) 314.
- [68] M. Baker, J.S. Ball, N. Brambilla, G.M. Prosperi and F. Zachariasen, *Phys. Rev. D* **54** (1996) 2829; N. Brambilla and A. Vairo, *Phys. Rev. D* **56** (1997) 1445.

- [69] P. Maris and P.C. Tandy, Phys. Rev. **C 61** (2000) 45202.
- [70] P. Maris and P.C. Tandy, "The  $\pi$ ,  $K^+$ , and  $K^0$  electromagnetic form factors," nucl-th/0005015.
- [71] P. Maris, these proceedings.
- [72] V.A. Miransky, Dynamical Symmetry Breaking in Quantum Field Theories (World Scientific, Singapore, 1993) pp. 202-207; H.J. Munczek, Phys. Rev. **D 52** (1995) 4736.
- [73] P. Maris and C.D. Roberts, Phys. Rev. **C 58** (1998) 3659.
- [74] C.D. Roberts, Nucl. Phys. **A 605** (1996) 475.
- [75] C.J. Bebek *et al.*, Phys. Rev. **D 13** (1976) 25.
- [76] S.R. Amendolia *et al.* [NA7 Collaboration], Nucl. Phys. **B 277** (1986) 168.
- [77] C.J. Bebek *et al.*, Phys. Rev. **D 17** (1978) 1693.
- [78] P. Maris and C. D. Roberts, "QCD bound states and their response to extremes of temperature and density," in Proc. of the Workshop on Non-perturbative Methods in Quantum Field Theory, edited by A.W. Schreiber, A.G. Williams and A.W. Thomas (World Scientific, Singapore, 1998) pp. 132-151.
- [79] J.M. Flynn and C.T. Sachrajda, Preprint hep-lat/9710057.
- [80] M. Oettel and R. Alkofer, Phys. Lett. **B 484** (2000) 243.
- [81] J.C.R. Bloch, Yu.L. Kalinovsky, C.D. Roberts and S.M. Schmidt, Phys. Rev. **D 60** (1999) 111502.
- [82] R.T. Cahill, C.D. Roberts and J.P. Opie, "A Derivation Of Hadron Soliton Phenomenology From QCD," preprint no. FIAS-R-158 (1985); J. Praschifka, C.D. Roberts and R.T. Cahill, Phys. Rev. **D 36** (1987) 209; C.D. Roberts, R.T. Cahill and J. Praschifka, Annals Phys. **188** (1988) 20; C. D. Roberts, J. Praschifka and R. T. Cahill, Int. J. Mod. Phys. **A 4** (1989) 1681; M. Bando, M. Harada and T. Kugo, Prog. Theor. Phys. **91** (1994) 927; R. Alkofer and C.D. Roberts, Phys. Lett. **B 369** (1996) 101; D. Kekez and D. Klabučar, Phys. Lett. **B 457** (1999) 359; D. Klabučar and D. Kekez, Fizika **B 8** (1999) 303. C.D. Roberts, Fizika **B 8** (1999) 285; P.C. Tandy, *ibid* 295; B. Bistrovic and D. Klabučar, Phys. Lett. **B 478** (2000) 127.
- [83] G. Hellstern, R. Alkofer, M. Oettel and H. Reinhardt, Nucl. Phys. **A 627** (1997) 679.
- [84] R.T. Cahill, C.D. Roberts and J. Praschifka, Austral. J. Phys. **42** (1989) 129; R.T. Cahill, Austral. J. Phys. **42** (1989) 171.
- [85] J.C.R. Bloch, C.D. Roberts, S.M. Schmidt, A. Bender and M.R. Frank, Phys. Rev. **C 60** (1999) 062201; M. Oettel, S. Ahlig, R. Alkofer and C. Fischer, "Form factors of baryons in a confining and covariant diquark-quark model," nucl-th/9910079; R. Alkofer, S. Ahlig, C. Fischer and M. Oettel, nucl-th/9911020,  $\pi N$  Newslett. No. **15** (1999) 238; J.C.R. Bloch, C.D. Roberts and S.M. Schmidt, Phys. Rev. **C 61** (2000) 065207; M.B. Hecht, C.D. Roberts and S.M. Schmidt, "DSE Hadron Phenomenology," nucl-th/0005067, to appear in Proc. of the Workshop on Light-Cone QCD and Nonperturbative Hadron Physics, Adelaide, Australia, 13-22 Dec 1999.
- [86] A. Bender, D. Blaschke, Yu.L. Kalinovsky and C.D. Roberts, Phys. Rev. Lett. **77** (1996) 3724.
- [87] P. Maris, C.D. Roberts and S.M. Schmidt, Phys. Rev. **C 57** (1998) 2821; P. Maris, C.D. Roberts, S.M. Schmidt and P.C. Tandy, "T-dependence of pseudoscalar and scalar correlations," nucl-th/0001064; P.C. Tandy, these proceedings.